

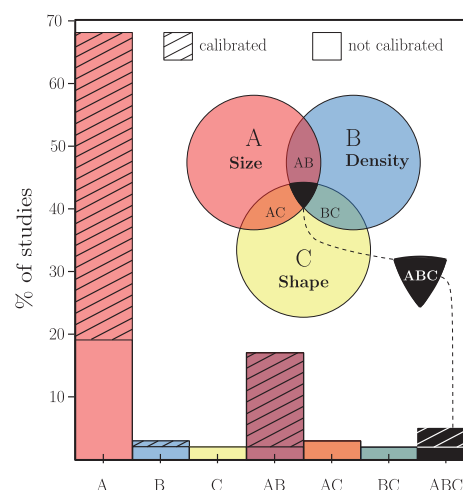
## DEM Modelling of Segregation in Granular Materials: A Review<sup>†</sup>

Ahmed Hadi<sup>‡</sup>, Raïsa Roepal<sup>‡</sup>, Yusong Pang and Dingena L. Schott<sup>\*</sup>

Department of Maritime and Transport Technology, Faculty of Mechanical Engineering, Delft University of Technology, The Netherlands

Segregation control is a challenging yet crucial aspect of bulk material handling processes. The discrete element method (DEM) can offer useful insights into segregation phenomena, provided that reliable models are developed. The main challenge in this regard is finding a good balance between including particle-level details and managing the computational load. This is especially true for industrial applications, where multi-component flows consisting of particles with various irregular shapes and wide size distributions are encountered in huge amounts. In this work, we review the state of the art in DEM modelling of segregation in industrial applications involving the gravity-driven flow of dry, cohesionless granular materials. We start by introducing a novel scientific notation to distinguish between different types of mixtures. Next, we review how parameters for mixture models are determined in the current literature, and how segregation is affected by material, geometric and operational parameters based on these models. Finally, we review existing segregation indices and their applicability to multi-component segregation. We conclude that systematic calibration procedures for segregation models are currently missing in the literature, and realistic models representing multi-component mixtures have not yet been developed. Filling these gaps will pave the way for optimising industrial processes dealing with segregation.

**Keywords:** segregation, granular materials, discrete element method, granular flow, DEM calibration



### 1. Introduction

Particulate materials are ubiquitous on Earth and are the second-most common materials handled in the industry (Richard et al., 2005). Nowadays, almost all commodities are composed of, and/or derived from granular materials through agriculture, mining, chemical, and/or mechanical processing (Coulson, 2012). Particulate materials being handled in the real world exhibit complex behaviour arising from the fact that almost all of them are either mixtures of different sizes, shapes, densities, or combinations thereof. Taking into account the market-driven demand for increasing production, lowering costs and the development of new sustainable products and systems, it is important to study and unravel the complex behaviour of granular materials, as well as to advance the technologies related to producing, processing, and transporting them (Rosato and Windows-Yule, 2020).

Segregation, also referred to as reverse mixing or de-mixing, is a phenomenon happening in moving granular

materials in which particles with similar properties, e.g., size, density and shape, tend to collect in certain parts of a mixture. Except for a few specific applications in mining and agricultural engineering (Zhang et al., 2004), segregation is generally considered an undesirable occurrence affecting product homogeneity in a negative way. A well-known example is the blast furnace, where segregation adversely influences the distribution of materials at the burden surface, which has a detrimental effect on the bed permeability (Yu and Saxén, 2010). This negative effect on permeability introduces an inconsistency in the pressure drop which leads to the inefficient use of reductant gas and resulting in both economic and environmental consequences (Bhattacharya and McCarthy, 2014). This example, along with several cases of other industries (e.g., food processing and pharmaceuticals industries) highlights the importance of increasing knowledge about the underlying roots of segregation, as well as investigating how segregation is influenced by various factors.

According to de Silva et al. (2000), there are thirteen segregation mechanisms in general. However, some of these mechanisms are either rare or special cases of others. Therefore, past researchers attempted to condense these segregation roots in different ways (Carson et al., 1986; Tang and Puri, 2004; Williams, 1991). Based on the size, Williams mentioned the four main mechanisms as

<sup>†</sup> Received 5 April 2023; Accepted 6 June 2023  
J-STAGE Advance published online 15 September 2023

<sup>‡</sup> Authors with equal contribution

<sup>\*</sup> Corresponding author: Dingena L. Schott;  
Add: Delft 2628 CD, The Netherlands  
E-mail: d.l.schott@tudelft.nl  
TEL: +31152783130

trajectory, percolation, the rise of coarse particles due to vibration (or Brazil-nut effect) and elutriation (Rhodes, 2008; Williams, 1991). In addition to these size-based mechanisms, the buoyancy mechanism in which the difference in density drives segregation should be considered for multi-component mixtures (Ottino and Khakhar, 2000). Having said that, multiple mechanisms might take place simultaneously, making the prediction of the segregation pattern extremely challenging. For instance, in the case of the mixture of small light and large heavy particles, percolation and buoyancy mechanisms oppose each other and the overall segregation behaviour of such a mixture is not known a priori (Jain et al., 2005). Furthermore, since segregation only occurs for particles that are in motion—due to either shearing, by means of moving walls (such as in a shear cell or bladed mixer) or as a result of gravitational force (as is the case in hoppers) or vibration—it can be deduced that the formation of segregation patterns depends not only on the properties of the components relative to each other, but also on the system configuration and the degree and type of agitation imposed on the material. Although having knowledge of the mentioned mechanisms can shed light on the segregation behaviour of particulate mixtures, it is necessary to investigate each case independently to determine the dominant segregation mechanism(s).

Researchers have attempted to experimentally observe segregation phenomena in common applications since the early '70s in order to first understand why and how granular mixture components tend to separate spatially during different types of agitation (Gray, 2018) and subsequently developed models capable of capturing the observed phenomena. Given the complexity of the segregation problem, the general approach was to scrutinize the effects of different material properties separately by considering material mixtures differing only in either size (Duffy and Puri, 2002) or density (Shlnohara and Mlyata, 1984) and, ultimately, the combined effect of size and density (Jain et al., 2005). This allowed researchers to systematically observe and incorporate the effect of each material property in mathematical models. However, there are several limitations associated with the experimental investigation of segregation. First, despite the recent advances in measurement techniques (Asachi et al., 2018; Bowler et al., 2020), extracting data on the composition of a granular mixture is still not a trivial task. Second, it is nearly impossible to obtain all the information on a particle scale which can shed light on the macro-scale granular behaviour. Finally, it is expensive and time-consuming to systematically study the effect of various factors on segregation in experiments.

As computational models gained popularity, the Discrete Element Method (DEM) initially introduced by Cundall and Strack (1979) became a widely used tool for simulating granular phenomena. The main advantage of DEM is that

any mixture of materials—whether they have different sizes, densities, shapes, or combinations thereof—can be modelled to provide detailed, particle-level insight on segregation patterns, which is both difficult and expensive to achieve experimentally and is not yet possible with mathematical models for segregation. This is highly relevant since most materials encountered in industry are of this complex nature. Hence, DEM has expedited researchers' ability to predict segregation in multi-component mixtures, irrespective of the application, and can therefore be considered a practical tool for modelling and optimising industrial processes. However, until now it is unclear to what extent the existing DEM models of segregation are representative of the complex multi-component mixtures often encountered in real-world applications. Moreover, a DEM model can accurately represent granular material behaviour only if its parameters are reliably chosen, i.e., the model is calibrated and validated.

The objective of this paper is to provide an overview of the state of the art in modelling the segregation behaviour of complex multi-component mixtures using DEM. Specifically, this review assesses to what extent the existing DEM studies of segregation in cohesionless materials represent actual mixtures encountered in industry. Furthermore, the reliability of these existing studies in terms of their approach to calibration and validation is evaluated. The paper is structured as follows. For the sake of consistency, a novel way of defining and using consistent terminology for the description of mixtures is proposed in [Section 2](#). Then in [Section 3](#), we first evaluate different ways of analysing segregation employed by past studies including their applicability to multi-component mixtures. Next, the approach of past DEM studies on segregation for determining DEM parameters is critically reviewed. Thereafter, an overview of the methods used for the validation of DEM models of segregation is presented and evaluated. Finally, the results of past DEM studies on the effect of several factors on segregation in different systems are reviewed in [Section 4](#). [Section 5](#) concludes the review and provides recommendations for future work.

The scope of this paper is limited to DEM-based studies of gravity-driven segregation of dry and cohesionless granular materials. Cohesionless (or free-flowing) granular materials are of interest because they are more susceptible to segregation compared to cohesive particles (Schulze et al., 2008). Studies on fluidised segregation are excluded since investigating such a phenomenon is conducted using the coupled CFD-DEM approach, which does not fit in this review. Also, applications such as rotating drums and various types of mixers in which gravity is not the only source of energy causing segregation are beyond the scope of this review.

## 2. Terminology

For consistency and to make a clear distinction between various terminologies used in this paper regarding mixtures, Fig. 1 is presented. In this figure, a component is defined as a material with constant particle density. In case a mixture is composed of more than one component, it is generically referred to as a multi-component or more specifically, as two-component, three-component, etc. by mentioning the exact number of components. Moreover, the particles constituting each component can be mono- to poly-sized and/or mono- to multi-shaped. In this regard, referring to complex mixtures composed of several components is not yet straightforward. To overcome this issue, we present in Eqn. (1) a novel way to define multi-component mixtures:

$$nC \left[ \sum_{k=1}^n (i_k S / j_k Sh) \right] \tag{1}$$

where  $n$  is the number of components and the composition of each component is specified in the corresponding parenthesis. That is,  $i_k$  is the number of sizes in  $k$ th component which could be 1, 2, 3,  $M$  or  $P$  representing a mono-, binary-, ternary-, multi- or poly-sized component. Similarly representing the shape,  $j_k$  might take the value of 1, 2, 3 or  $M$  denoting a mono-, binary-, ternary- or multi-shaped component. For instance,  $2C[(2S/1Sh) + (MS/1Sh)]$  represents a two-component ( $2C$ ) mixture composed of a binary-sized ( $2S$ ) mono-shaped ( $1Sh$ ) component mixed with a multi-sized ( $MS$ ) mono-shaped ( $1Sh$ ) one. This formula will be consistently used in this review to refer to different types of mixtures in a concise way.

## 3. Discrete element method (DEM) for segregation

### 3.1 Overview of DEM

A DEM model calculates the forces and moments of inertia acting on all particles and subsequently uses Newton’s second law to compute their positions at each time step through numerical integration. The interaction forces between particles and their surroundings are determined using contact models such as the Linear spring-dashpot (Luding, 2008) and Hertz-Mindlin model (Zhu et al., 2007), which are the most widely used for cohesionless granular materials. The model inputs can generally be divided into three categories: (i) morphological parameters such as particle size and shape distributions; (ii) material parameters such as particle density ( $\rho$ ), shear modulus ( $G$ ) and Poisson ratio ( $\nu$ ); and (iii) interaction parameters such as sliding and rolling friction coefficients ( $\mu_s$  and  $\mu_r$ , respectively) and the restitution coefficient (CoR).

The first step in developing a DEM model is generally measuring morphological parameters, and determining how they will be included in the model. In industrial applications, millions of particles with many irregular shapes and wide size distributions are typically handled. From a computational standpoint, modelling the true size and shape distributions for such applications can be very challenging for several reasons (Marigo and Stitt, 2015; Roessler and Katterfeld, 2018; Sakai, 2016). First of all, tracking a large number of particles and their mutual interactions demands huge amounts of computational power, even for simulating a few seconds of a simple process. Secondly, modelling the actual size distribution can prolong simulation times significantly since the numerical time step is determined by the smallest particle in the flow. Finally, realistic (non-spherical) particle shapes can be

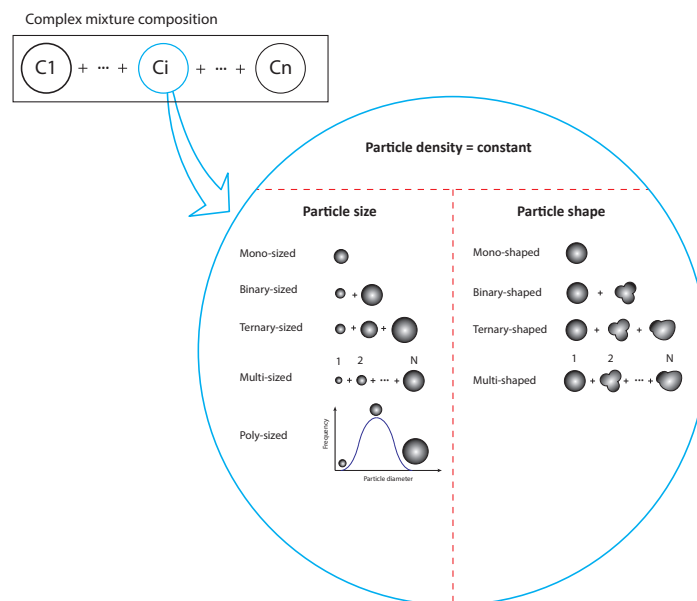


Fig. 1 Terminology to describe various types of mixtures.

modelled using multi-spheres or superquadrics which require computationally expensive algorithms (Soltanbeigi et al., 2018). Several solutions have been proposed to reduce computational effort such as downscaling the full three-dimensional system to a 2D representation or simulating a portion using periodic boundaries (Yang et al., 2014; 2015) using larger, so-called “coarse-grained” or “upscaled” particles (Coetzee, 2019; Lommen et al., 2019; Roessler and Katterfeld, 2018), ignoring small sizes of the full particle size distribution (PSD—also referred to as “scalping” or “cut-off” (Cleary and Sawley, 2002)—and reducing the shear modulus ( $G$ ), although the latter should be carried out with caution as it might cause serious errors (Lommen et al., 2014). Besides all these techniques, DEM code development in conjunction with parallel computing techniques using high-performance clusters (HPC) look promising to overcome the high computational time in due course (Marigo and Stitt, 2015).

The next step is determining the remaining model parameters such that the simulated flow behaviour matches the real behaviour to an acceptable degree (Marigo and Stitt, 2015). When it comes to modelling segregation, the parameters should be determined in a way that not only the

global behaviour (e.g., angle of repose, mass flow rate, etc.) but also the local behaviour, i.e., spatial concentration of components, are captured. The reliability of DEM predictions depends on the proper selection of a contact model for a specific application and the values assigned to the model parameters, given the simplifications which have been made for computational reasons. Model validation is therefore an important final step for both verifying and demonstrating the model’s credibility.

We encountered 63 papers on the segregation of the gravity-driven flow of cohesionless granular materials in the literature. These studies are mostly focused on segregation during hopper filling and discharge, chute flow and heap formation and are summarised in **Table 1**. These studies have been categorised into four groups based on their approach to obtaining DEM parameters. In the remainder of this section, we will review the studies from **Table 1** with respect to the methods used to quantify segregation (**Section 3.2**) and model development practices (**Sections 3.3 and 3.4**).

### 3.2 Methods for assessing segregation

Since DEM allows tracking the position of each

**Table 1** Overview of DEM studies for segregation (LSD = Linear spring dashpot, HM = Hertz-Mindlin, n.s. = not specified, N/A = not applicable, \*for the definition and notation of the mixture type see **Eqn. (1)** in **Section 2**). (continued on next page)

Group	Source	Software	Contact model	Mixture type*	Material (in experiments)	Particle shape
I. Parametric sensitivity studies	(Tripathi and Khakhar, 2011; 2013)	n.s.	LSD	$1C[(2S/1Sh)]$ $2C[(1S/1Sh) + (1S/1Sh)]$	N/A	Sphere
	(Ketterhagen et al., 2008)	n.s.	LSD	$1C[(2S/1Sh)]$ $2C[(1S/1Sh) + (1S/1Sh)]$		Sphere
	(Pereira and Cleary, 2013)	n.s.	LSD	$2C[(1S/1Sh) + (1S/1Sh)]$		Sphere
	(Panda and Tan, 2020a; 2020b)	LIGGGHTS	HM	$1C[(2S/1Sh)]$ $2C[(1S/1Sh) + (1S/1Sh)]$		Sphere
	(Huang et al., 2022)	n.s.	n.s.	$1C[(2S/1Sh)]$		Sphere
	(Yu and Saxén, 2014)	EDEM	HM	$1C[(3S/1Sh)]$		Sphere
	(Xu et al., 2019)	n.s.	HM	$3C[(MS/1Sh) + (MS/1Sh) + (MS/1Sh)]$		Sphere
	(Li et al., 2022)	n.s.	HM	$2C[(2S/1Sh) + (2S/1Sh)]$		Sphere
	(Vuilloz et al., 2021)	LMGC90	n.s.	$1C[(2S/1Sh)]$		Sphere
	(Zhao et al., 2022)	PFC3D	LSD	$1C[(3S/1Sh)]$		Sphere
II. Parameter assumption	(Tao et al., 2013)	n.s.	n.s.	$1C[(2S/2Sh)]$	Soybean	Ellipsoidal, corn-shaped, cylinder, spherical
	(Shirsath et al., 2015)	n.s.	LSD	$2C[(1S/1Sh) + (1S/1Sh)]$	Glass beads	Sphere
	(Xu et al., 2017)	n.s.	n.s.	$1C[(2S/1Sh)]$	Alumina spheres	Sphere
	(Zhang et al., 2018)	n.s.	HM	$1C[(2S/1Sh)]$	Plastic pellets, rape seeds	Sphere
	(Mantravadi and Tan, 2020)	LIGGGHTS	HM	$1C[(2S/1Sh)]$	Glass beads	Sphere
	(Mio et al., 2020)	n.s.	Voigt	$1C[(MS/1Sh)]$	Sintered ore, coke	Sphere
	(Zhang et al., 2014)	n.s.	HM	$1C[(MS/1Sh)]$	Coke, iron ore	Sphere
	(Zhao et al., 2018)	LIGGGHTS	HM	$1C[(PS/1Sh)]$	Glass beads	Sphere
	(Zhao and Chew, 2020b)	LIGGGHTS	HM	$1C[(PS/1Sh)]$	Glass particles	Sphere, ellipsoid, cylinder, cuboid
	(Kumar et al., 2020)	LIGGGHTS	HM	$1C[(PS/1Sh)]$	Glass beads	Sphere

**Table 1** Overview of DEM studies for segregation (LSD = Linear spring dashpot, HM = Hertz-Mindlin, n.s. = not specified, N/A = not applicable, \*for the definition and notation of the mixture type see Eqn. (1) in Section 2). (continued from previous page)

Group	Source	Software	Contact model	Mixture type*	Material (in experiments)	Particle shape
III. Parameters from literature	(Ketterhagen et al., 2007; 2009)	n.s.	LSD	$1C[(2S/1Sh)]$ $2C[(1S/1Sh) + (1S/1Sh)]$	Glass beads, cast steel shot	Sphere
	(Ketterhagen and Hancock, 2010)	n.s.	LSD	$1C[(2S/1Sh)]$	Glass beads	Sphere
	(Kou et al., 2015; 2018)	n.s.	HM	$4C[(1S/1Sh) + (1S/1Sh) + (1S/1Sh) + (1S/1Sh)]$	Pellet, ore, coke, flux	Sphere
	(Cliff et al., 2021)	MFiX	LSD	$1C[(2S/1Sh)]$	Mustard seed	Sphere
	(Yu and Saxén, 2013)	EDEM	HM	$1C[(2S/1Sh)]$	Pellet	Sphere
	(Liao et al., 2023)	n.s.	n.s.	$2C[(1S/1Sh) + (1S/1Sh)]$	Lump ore, pellet	Sphere, clumped spheres
	(Asachi et al., 2021)	EDEM	HM	$3C[(1S/1Sh) + (1S/1Sh) + (1S/1Sh)]$	TAED, BP, EPG (detergent powder)	Sphere, clumped spheres
	(Tian et al., 2022)	n.s.	HM	$1C[(3S/1Sh)]$	Coke	Sphere, clumped spheres
	(Yu et al., 2018)	EDEM	HM	$1C[(2S/1Sh)]$	Pellet	Sphere
	(Xu et al., 2018b)	n.s.	HM	$1C[(2S/1Sh)]$	Mung bean	Sphere
	(Mandal and Khakhar, 2019)	n.s.	LSD	$1C[(2S/1Sh)]$	N/A	Spheres, dumbbells
	(Zhao and Chew, 2020a)	LIGGGHTS	HM	$1C[(1S/2Sh)]$	N/A	Ellipsoids, cylinders, cuboids
	(Zhang et al., 2021)	n.s.	HM	$1C[(2S/1Sh)]$	Coke	Sphere
	(Yu and Saxén, 2010)	EDEM	HM	$1C[(3S/1Sh)]$	Pellets	Sphere
	(Yu and Saxén, 2012)	EDEM	HM	$1C[(3S/1Sh)]$	Pellets, coke, steel ball	Sphere, clumped spheres
	(Kou et al., 2013)	n.s.	Voigt	$1C[(3S/1Sh)]$	Coke	Sphere
	(Wu et al., 2013)	n.s.	HM	$1C[(3S/1Sh)]$	Sinter	Sphere
	(You et al., 2016)	n.s.	HM	$1C[(3S/1Sh)]$	Coal	Sphere
	(Xu et al., 2021)	n.s.	n.s.	$1C[(MS/1Sh)]$	Coke	Sphere
	(Kou et al., 2019)	n.s.	HM	$3C[(1S/1Sh) + (1S/1Sh) + (1S/1Sh)]$	Sinter, pellet, lump ore	Sphere
(Chibwe et al., 2020)	LIGGGHTS	HM	$2C[(MS/1Sh) + (1S/1Sh)]$	Sinter, pellet	Sphere	
(Hong et al., 2021)	n.s.	HM	$3C[(1S/1Sh) + (1S/1Sh) + (1S/1Sh)]$	Sinter, pellet, ore	Sphere	
IV. Parameter calibration/ measurement	(Z. Zhang et al., 2020)	EDEM	HM	$1C[(2S/1Sh)]$	Acrylic spheres	Sphere
	(Izard et al., 2021)	EDEM	HM	$1C[(2S/1Sh)]$	Sinter	Clumped spheres
	(Alizadeh et al., 2017)	EDEM	HM	$2C[(1S/1Sh) + (1S/1Sh)]$	TAED, BP (detergent powder)	Clumped spheres
	(Kim et al., 2020)	EDEM	HM	$2C[(3S/1Sh) + (3S/1Sh)]$	Sinter, briquette	Sphere, clumped sphere
	(Qiu and Pabst, 2022)	PFC3D	LSD	$1C[(MS/1Sh)]$	Waste rock	Sphere
	(Wang et al., 2023)	LIGGGHTS	HM	$2C[(1S/1Sh) + (1S/1Sh)]$	Steel and aluminium spheres	Sphere
	(Barik et al., 2023)	LIGGGHTS	HM	$1C[(3S/1Sh)]$	Microcrystalline cellulose (MCC)	Sphere
	(Mio et al., 2008a; 2009; 2010; 2012)	n.s.	Voigt	$1C[(3S/1Sh)]$	Sintered ore	Sphere
	(Nakano et al., 2012)	n.s.	Voigt	$1C[(3S/1Sh)]$	Sinter	Sphere
	(Bhattacharya and McCarthy, 2014)	n.s.	HM	$1C[(3S/1Sh)]$	Polystyrene spheres	Sphere
	(Li et al., 2017)	n.s.	HM	$1C[(MS/1Sh)]$	Iron ore	Sphere
	(Li et al., 2019)	LIGGGHTS	HM	$1C[(MS/1Sh)]$	Iron ore	Sphere
	(Shimosaka et al., 2013)	n.s.	LSD	$1C[(MS/1Sh)]$	Glass bead, sand, alumina	Sphere
	(Combarros et al., 2014)	LIGGGHTS	HM	$1C[(2S/1Sh)]$ $2C[(1S/1Sh) + (1S/1Sh)]$	Aluminium oxide	Sphere, cylinders
	(Combarros et al., 2016)	LIGGGHTS	HM	$1C[(2S/1Sh)]$	Sand	Sphere
	(Terui et al., 2017)	n.s.	Voigt	$2C[(1S/1Sh) + (1S/1Sh)]$	Coke, sinter	Sphere

individual particle, it becomes relatively simple to assess the degree of segregation within a system. This can be done in different ways. One approach is to divide the system into subdomains and subsequently determine how different mixture components are distributed in the subdomains by means of plots. Gradient plots are useful for visualising the distribution of a single mixture component in a system. For example, a gradient plot as in Fig. 2(a) has been used to visualise how small particles within a binary mixture were distributed after filling a hopper (Xu et al., 2017). Since they were dealing with a binary mixture, showing the distribution of one component was sufficient to demonstrate how well the material was mixed in the hopper. When dealing with multi-component mixtures, monitoring only one component's distribution is no longer sufficient, and other types of plots can be used. Fig. 2(b) shows an example of line plots for monitoring the radial distribution of four different particle sizes in a blast furnace. The method of plots is beneficial as it provides two important insights: (1) whether or not different mixture components are evenly distributed and (2) where the different components are concentrated in the case of uneven distribution.

Another method is to use an index which reflects the degree of segregation based on its value. There are generally two types of segregation indices: grid-dependent and grid-independent (Bhalode and Ierapetritou, 2020). In the first type, the system is divided into subdomains, similar to the method of plots. The distribution of one mixture component (referred to as the tracer) is evaluated, and the segregation index is then determined through statistical

analysis of the tracer distribution. If the tracer is distributed evenly, then the material is considered to be well-mixed, and this is reflected by the value of the segregation index. In the second type, the value of the segregation index is determined by considering how the tracer particle is distributed within the system as a whole, rather than in subdomains. The tracer's distribution is generally evaluated on a distance or contact basis, as described by Bhalode and Ierapetritou (2020). The index value reflects how spread out the tracer particles are in the whole system.

The benefit of using an index is that it allows for a quantitative comparison of segregation for different scenarios by means of a single value. This might be more difficult to do with the method of plots, which provides a more qualitative comparison. However, it is generally known that grid-dependent indices depend on the chosen size of the subdomains (Cho et al., 2017; Jin et al., 2022; Rosato and Windows-Yule, 2020), which makes it difficult to judge the degree of segregation based on the index value. For this reason, researchers often investigate how sensitive their segregation predictions are to the grid size. While the grid-independent indices do not have this shortcoming, they are often computationally intensive, especially for industrial applications where millions of particles are involved.

The majority of literature from Table 1 used the plot method to quantify segregation, with only a few used segregation indices. These indices are presented in Table 2 and are grouped by the calculation method (grid dependent/independent). The equations for calculating the indices are

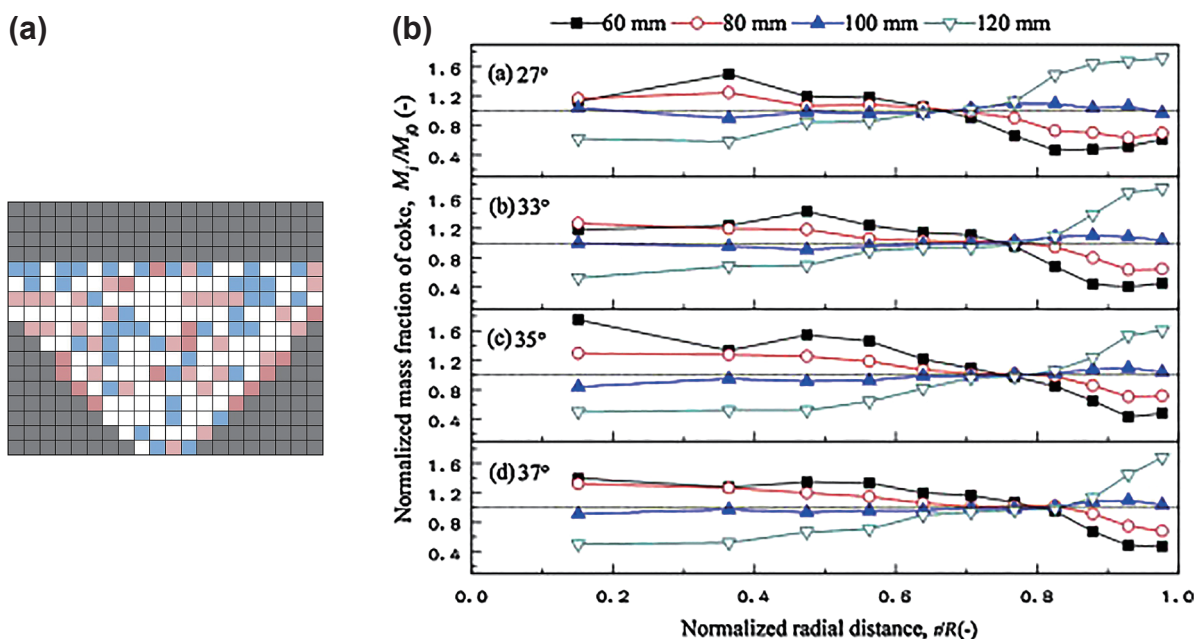


**Fig. 2** (a) Gradient plot for demonstrating how a single component is spatially distributed inside a system, where white colour represents a well-mixed status and red and blue colours denote segregated areas. Reproduced with permission from Ref. (Xu et al., 2017). Copyright 2017, Elsevier. and (b) line plots for different coke sizes, showing how they are distributed inside a blast furnace after being charged using various chute angles. Reproduced with permission from Ref. (Zhang et al., 2014). Copyright 2014, Elsevier.

**Table 2** Common segregation indices used in DEM studies of **Table 1**. Legend: refer to the **Appendix** for symbol definitions. Subscripts: “t” refers to “tracer” when a single tracer is used;  $t_i$  refers to the  $i$ -th tracer when multiple tracers are used<sup>(\*)</sup>.

No.	Source	Segregation index	Values (mixed-segregated)	Classification
<b>Grid-dependent</b>				
1	(Panda and Tan, 2020a; 2020b)	$SI = \sqrt{\frac{\sum_{j=1}^m (c_t^j - c_t)^2}{m}}$	0–(**)	Variance-based / single tracer
2	(Li et al., 2022)	$SI = \frac{\sum_{j=1}^m \left[ \frac{N^j}{N} (y_t^j - y_t)^2 \right]}{y_t (1 - y_t)}$	0–1	Variance-based / single tracer
3	(Mantravadi and Tan, 2020)	$SI = \sqrt{\frac{\sum_{j=1}^m \left[ \frac{x_t^j}{x_t} - \left( \frac{x_t^j}{x_t} \right)_{\text{avg.}} \right]^2}{m - 1}}$	0–(**)	Variance-based / single tracer
4	(Mantravadi and Tan, 2020)	$SI = \frac{\sigma_0^2 - \sigma^2}{\sigma_0^2 - \sigma_r^2}$	1–0(***)	Variance-based / single tracer
5	(Zhang et al., 2014), (Ketterhagen and Hancock, 2010)	$SI = \sqrt{\frac{\sum_{j=1}^m \left[ \frac{x_t^j}{x_t} - \left( \frac{x_t^j}{x_t} \right)_{\text{avg.}} \right]^2}{m}}$	0–(**)	Variance-based / single tracer
6	(Zhao et al., 2018)	$SI = \frac{\frac{\sum_{j=1}^m [x_{t_1}^j \cdot h_j]}{\sum_{j=1}^m [x_{t_2}^j \cdot h_j]} - 1}{\frac{2x_{t_2} + x_{t_1}}{x_{t_1}} - 1}$	0–1	Distance-based / two tracers
7	(Combarros et al., 2014)	$SI = \sqrt{\frac{\log \sigma_0^2 - \log \sigma^2}{\log \sigma_0^2 - \log \sigma_r^2}}$	1–0	Variance-based / single tracer
<b>Grid-independent</b>				
8	(Zhang et al., 2018)	$SI = \frac{\sigma_0^2 - \sigma^2}{\sigma_0^2 - \sigma_r^2}$ (*)	1–0	Contact-based
9	(Mandal and Khakhar, 2019)	$SI = \frac{COM_{\text{final}} - COM_{\text{initial}}}{\delta}$	0–0.5	Distance-based / single tracer
10	(Chibwe et al., 2020)	$SI = \frac{\bar{l} - l_{\min}}{l_{\text{ud}} - l_{\min}}$	1–0	Distance-based / single tracer

(\*) The readers are referred to **Table A1** in the **Appendix** for detailed equations on calculating component concentrations of indices 1–8.

(\*\*) For these indices, the maximum value of  $SI$  depends on the mixture composition, as the equations contain the variables  $c_t$ ,  $y_t$  and  $x_t$  which represent the concentration of the tracer in the entire mixture.

(\*\*\*) In these equations,  $\sigma^2$ ,  $\sigma_0^2$  and  $\sigma_r^2$  are calculated by

$$\sigma^2 = \sum_{i=1}^n \frac{(y_i^t - y_t)^2}{n - 1}, \sigma_0^2 = y_t (1 - y_t), \sigma_r^2 = \frac{y_t (1 - y_t)}{N^i}$$

given along with the range of values that can be assigned to each index. Additionally, the type of segregation index based on the classification according to Bhalode and Ierapetritou (2020) is indicated. It is important to note that, similar to the method of plots, the single-tracer approach is only useful when considering a binary mixture. We have therefore also indicated whether the segregation indices are based on the distribution of a single tracer. The common symbols used in index no. 1–8 from **Table 2** are defined in

the **Appendix**, and for index no. 9–10, the reader is referred to the respective references.

We conclude that all grid-dependent indices in **Table 2** are based on a statistical analysis of a single tracer, which is not surprising since they were applied to studies of binary mixtures. In studies of three or more particle types (Bhalode and Ierapetritou, 2020), the plot method was used to visualize the degree of segregation. For indices which can be applied to multi-component segregation, the reader

is referred to the work of Cho et al. (2017), who studied segregation in a mixer.

### 3.3 Determination of DEM parameters for segregation

The literature mentioned in **Table 1** has been categorized based on the way in which the authors dealt with model parameters. We identified the following four categories:

I. **Parametric sensitivity studies.** This group of studies carried out parametric sensitivity studies to identify the critical factors (i.e., model, material, geometric and operational parameters) affecting the segregation behaviour of mixtures in different systems. Hence, parameter values in these studies are systematically varied. Since they are not aimed at modelling a specific material, calibration and validation are not performed in these studies.

II. **Parameter assumption.** The second group contains studies in which the authors assumed parameters without any justification or referring to related resources (for instance chosen by experience). Although these studies attempted to justify the parameter values by comparing the DEM results with physical tests, this is insufficient because more than one parameter set can yield the same bulk behaviour (Roessler et al., 2019). Furthermore, major errors were reported in some cases (Tao et al., 2013), which could be the consequence of not calibrating the parameters.

III. **Parameters from literature.** Many DEM studies on segregation have taken either all or merely a selection of the parameters from the literature (Asachi et al., 2021; Chibwe et al., 2020; Cliff et al., 2021; Hong et al., 2021; Ketterhagen et al., 2007, 2009; Ketterhagen and Hancock, 2010; Kou et al., 2013, 2015, 2018, 2019; Liao et al., 2023; Mandal and Khakhar, 2019; Tian et al., 2022; Wu et al., 2013; Xu et al., 2018b, 2021; You et al., 2016; Yu et al., 2018; Yu and Saxén, 2010, 2012, 2013; Zhang et al., 2021; Zhao and Chew, 2020a). This approach has the same shortcoming as the previous group, since the parameters are obtained from resources that have not conducted calibration. Furthermore, it is unclear if the material under study is similar or exactly the same as in the literature (Zhang et al., 2021).

IV. **Parameter calibration/ measurement.** Several past

studies have established DEM parameters through either direct measurements or bulk calibration (Alizadeh et al., 2017; Barik et al., 2023; Bhattacharya and McCarthy, 2014; Combarros et al., 2014; Combarros Garcia et al., 2016; Izard et al., 2021; Kim et al., 2020; Li et al., 2019, 2017; Mio et al., 2010, 2009, 2008a, 2012; Nakano et al., 2012; Qiu and Pabst, 2022; Shimosaka et al., 2013; Terui et al., 2017; Wang et al., 2023; Z. Zhang et al., 2020). Each of these approaches comes with a set of advantages and disadvantages as summarized in **Table 3**. The calibration approaches of the studies in this group are summarized in **Table 4**. All calibration tests presented in this table capture only the global behaviour of granular materials (e.g., angle of repose) and none of them has calibrated the DEM model for local behaviour using a segregation test.

Calibration of DEM models against experimental data ensures that the model captures the material behaviour and therefore provides credibility (Coetzee, 2017). However, calibration can be very time-consuming. This is especially true for multi-component mixtures since the number of model parameters increases with the number of components in the mixture. Sensitivity studies enable us to explore the importance of the model parameters for inclusion in the calibration step. **Table 5** presents a summary of the results of the existing DEM sensitivity studies on segregation. As can be seen, the significance of DEM parameters depends on the system and the granular flow regime being studied.

**Fig. 3** visually presents deeper insight into studies listed in **Table 1** to highlight the percentage of studies with respect to the approach for determining DEM parameters, reproducibility and the types of the mixtures being studied.

According to **Table 1**, not all past DEM studies have determined the parameters in a proper way. To highlight this with respect to segregation, **Fig. 3(a)** shows the percentage of studies in groups II to IV, where only studies in group IV include calibration. It should be noted that group I is excluded since calibration is not necessary for parametric sensitivity analysis. As can be seen, 66 % of the existing studies have omitted the calibration of the DEM model. This is relevant since calibrated DEM models are required if they are intended to be used as predictive tools that yield

**Table 3** Pros and cons of two main approaches to determining DEM parameters (Coetzee, 2017; Marigo and Stitt, 2015; Wang et al., 2022).

	Advantage	Disadvantage
Direct measurement	<ul style="list-style-type: none"> <li>+ Independent of the contact model</li> <li>+ Independent of the DEM code</li> <li>+ Maintaining physical meaning</li> </ul>	<ul style="list-style-type: none"> <li>– Mostly limited to mm-sized particles</li> <li>– Not practical for irregular particles</li> <li>– Not practical for all parameters</li> <li>– Not considering the stochastic nature of the parameters</li> </ul>
Bulk Calibration	<ul style="list-style-type: none"> <li>+ Compensating for the inaccuracy of the parameters</li> <li>+ Obtaining values for all parameters</li> </ul>	<ul style="list-style-type: none"> <li>– Probability of losing physical meaning on particle level</li> <li>– DEM code dependency</li> <li>– Probability of not resulting in a unique parameter set</li> <li>– Challenging in the case of a high number of parameters</li> </ul>

**Table 4** Detailed calibration approach of studies in group IV of Table 1.

Source	Direct measurement	Bulk calibration test
(Z. Zhang et al., 2020)	$\mu_{s,pp}, \mu_{s,pw}, \text{CoR}$	—
(Izard et al., 2021)	$\mu_{s,pw}, \rho_s$	$\mu_{s,pp}$ (angle of repose)
(Alizadeh et al., 2017)	CoR, $\mu_{s,pw}$ , particle shape	The number of spheres in clumped approach, $\mu_r$ (angle of repose), $\mu_{s,pp}$ (sliding process),
(Kim et al., 2020)	PSD, $\rho_s$ , CoR, $\mu_s$ , E	$\mu_r$ (angle of repose)
(Qiu and Pabst, 2022)	PSD	$\mu_s, \mu_r$ (angle of repose, both at lab and field scales)
(Wang et al., 2023)	$\rho_s$ , CoR	—
(Barik et al., 2023)	—	$\mu_s$ (silo discharging)
(Mio et al., 2008a; 2009; 2010; 2012)	PSD, $\rho_s$	$\mu_s$ (shear test), $\mu_r$ (particle rolling test)
(Nakano et al., 2012)	—	$\mu_r$ (angle of movement)
(Bhattacharya and McCarthy, 2014)	PSD, $\rho_s$	Tuning the contact model
(Li et al., 2017)	PSD, $\rho_s$ , G	$\mu_s, \mu_r$ (angle of repose)
(Li et al., 2019)	PSD, $\rho_s$ , G, $\mu_s, \mu_r$	—
(Shimosaka et al., 2013)	—	$\mu_r$ (inclined plate test)
(Combarros et al., 2014)	PSD, $\rho_s$	$\mu_s, \mu_r$ (sensitivity analysis + dynamic and static angle of repose)
(Combarros Garcia et al., 2016)	$\rho_s, D_{50}$	$\mu_s$ , CoR (sensitivity analysis + shear test, angle of repose and drop fall test)
(Terui et al., 2017)	—	$\mu_s$ (stationary bed angle), $\mu_r$ (angle of repose)

**Table 5** A summary of the results of DEM sensitivity studies on the significance of model parameters for segregation.

DEM parameter	Range (source)	System	Significance
Particle-particle sliding friction ( $\mu_{s,p-p}$ )	(0.0–0.5) (Ketterhagen et al., 2008)	Hopper discharge	High
	(0.01–0.9) (Yu and Saxén, 2010)		Low
	(0.15–0.95) (Z. Zhang et al., 2020)		High
	(0.1–1.0) (Zhang et al., 2018)	Hopper filling	High
	(0.3–0.9) (Li et al., 2022)	Blast furnace throat	Low
Particle-wall sliding friction ( $\mu_{s,p-w}$ )	(0.0–0.5) (Ketterhagen et al., 2008)	Hopper discharge	High
	(0.01–0.9) (Yu and Saxén, 2010)		High
	(0.05–0.85) (Z. Zhang et al., 2020)		High
Particle-particle rolling friction ( $\mu_{r,p-p}$ )	(0.0–0.045 $d_c$ ) (Ketterhagen et al., 2008)	Hopper discharge	Low
	(0.05–0.9) (Yu and Saxén, 2010)		Low
	(0.001 $d_p$ –0.2 $d_p$ ) (Zhang et al., 2018)	Hopper filling	High
Particle-wall rolling friction ( $\mu_{r,p-w}$ )	(0.0–0.045 $d_c$ ) (Ketterhagen et al., 2008)	Hopper discharge	Low
	(0.01–0.9) (Yu and Saxén, 2010)		High
Particle-particle coefficient of restitution ( $e_{p-p}$ )	(0.2–0.94) (Ketterhagen et al., 2008)	Hopper filling	High
Particle-wall coefficient of restitution ( $e_{p-w}$ )	(0.2–0.9) (Ketterhagen et al., 2008)	Hopper filling	High
Local damp	(0.2–0.8) (Qiu and Pabst, 2022)	Pile formation	Low

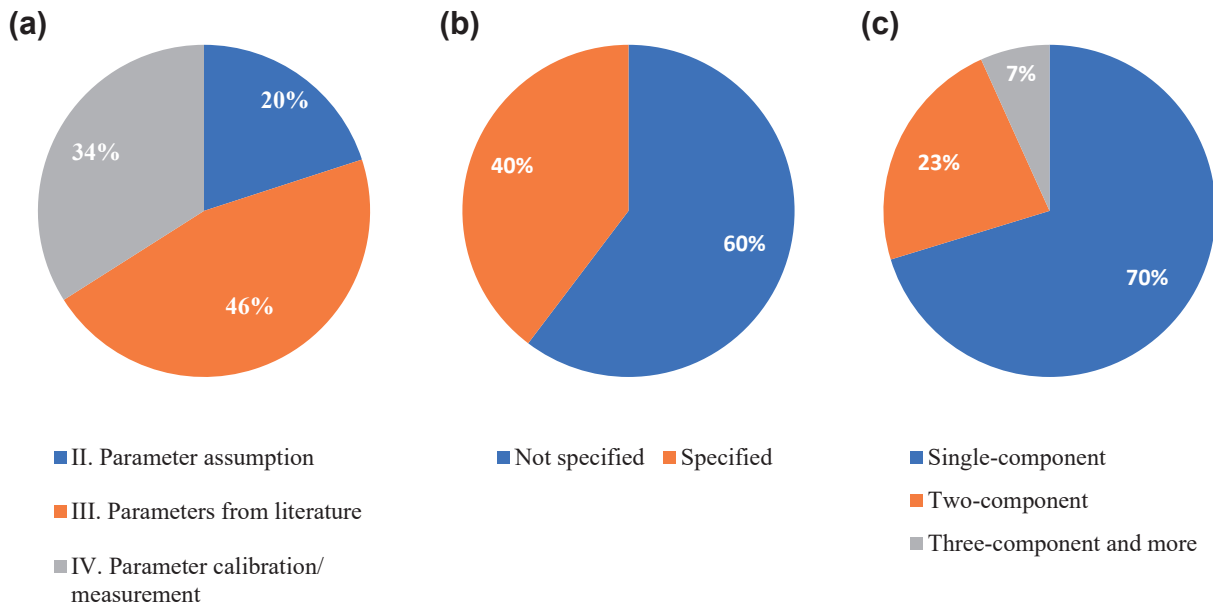


**Fig. 3** Distribution of past DEM-based studies of segregation by (a) approach of calibration, (b) DEM software and (c) types of mixtures.

reliable results (Coetzee, 2017). Even though the studies in group IV have applied calibration to some extent, not all of them have carried it out in a systematic way (cf. **Table 4**). In several studies, only a portion of the parameters has been calibrated (Nakano et al., 2012; Shimosaka et al., 2013). Also, in several cases, a single experiment is used to determine the values of more than one parameter (Izard et al., 2021; Li et al., 2017). As shown by Wensrich and Katterfeld (2012), this approach leads to ambiguity since an infinite combination of parameter values might lead to the same bulk behaviour.

There are good examples of systematic calibration of DEM models with respect to bulk material behaviour for various operational conditions in the literature (Coetzee, 2016; Do et al., 2018; El Kassem et al., 2021; Marigo and Stitt, 2015; Mohajeri et al., 2020; Roessler et al., 2019). When it comes to the calibration of models for segregation, several authors have shown that bulk calibration also ensures that the local material behaviour is accurately captured. For example, Li et al. (2017) calibrated the friction coefficients of iron ore pellets using a repose angle test and verified that the calibrated model could reproduce the experimentally observed size segregation in simulations. Similarly, Izard et al. (2021) modelled the size segregation of sinter particles after determining the model parameters through bulk calibration. However, it has not yet been addressed to what extent the DEM parameters obtained through bulk calibration (e.g., dynamic and static angle of repose) can be employed to accurately replicate the segregation of multi-component mixtures, which is essentially a local occurrence. Furthermore, the systematic calibration of mixture models has received little attention. One of the few studies where mixture calibration was performed is the

work of Alizadeh et al. (2017). The authors modelled the segregation of a detergent mixture during heap formation and found that the segregation behaviour was not accurately captured by their model, which was calibrated using a combination of direct measurement and bulk calibration. They attributed the model's inaccuracy to the fact that spheres were used to model the particle shape. When using clumped spheres to approximate the actual particle shape, the predicted segregation behaviour was in good agreement with the experiments. Other researchers have also modelled the segregation of mixtures, but the interaction parameters between mixture components were not mentioned (Combarros et al., 2014; Terui et al., 2017).

**Fig. 3(b)** illustrates the various DEM software that has been used by past researchers to investigate segregation. It is notable that 60 % of the studies have not specified the DEM software they employed. This is highly important because not only the same DEM parameters might be defined in different ways in various software, but also models may be differently implemented, making the parameters code-dependent (Coetzee, 2017; González-Montellano et al., 2012). It means that the calibrated parameters of these studies cannot be reliably and directly used by others to reproduce the work or to model the same material. Therefore, it is essential to specify in detail the DEM code or software used in future studies.

The different types of mixtures that have been modelled and studied are shown in **Fig. 3(c)**. A vast majority of past studies (i.e. 70 %) have been dedicated to single-component mixtures i.e., with the general form of  $1C[(iS/jSh)]$  (see **Section 2**), most of which have modelled simple binary- or ternary-sized mixtures with spherical particles (i.e.,  $1C[(2S/1Sh)]$  or  $1C[(3S/1Sh)]$ ). In addition, a few

studies considered two or three components (Chibwe et al., 2020; Combarros et al., 2014; Hong et al., 2021; Ketterhagen et al., 2007; Kou et al., 2019; Li et al., 2022; Panda and Tan, 2020a; Pereira and Cleary, 2013; Shirsath et al., 2015; Terui et al., 2017; Xu et al., 2019), but they also simplified the mixtures by modelling mono-sized and mono-shaped components. In conclusion, although past DEM studies have attempted to shed light on segregation in granular materials, they have failed to represent the real-world complex mixtures which are mostly multi-component with each component having a size distribution and different particle shapes (Gao et al., 2021).

As can be seen in **Table 1** (columns *Mixture type* and *Particle shape*), the particle shape and size distribution have often been simplified, mainly to prevent high computational time. The effect of particle shape on segregation is not crystal clear yet as can be illustrated by seemingly contradictory results in the literature. For instance, Yu and Saxén (2014) asserted that particle shape has an insignificant effect on the size segregation during charging and discharging from a hopper since spherical particles yielded the best agreement with the experimental results of Standish (1985). It is notable that they used the same DEM parameters for both spherical and non-spherical particles, which can lead to misinterpretation. In another study, Alizadeh et al. (2017) concluded that modelling non-spherical particles as spherical with rolling friction underestimates the segregation extent during heap formation. Despite this conflict, Lu et al. (2015) and Combarros Garcia et al. (2016) concluded that particle shape has to be modelled as accurately as possible to ensure that the DEM model is accurate and predictive. Similarly, particle size distribution has usually been approximated either by using a limited number of sizes or scalping (cf. **Section 3.1**). However, since particle size is the most crucial parameter affecting segregation (Williams, 1976), size distribution should be modelled as precisely as possible. As stated by Coetzee (2017), particle shape along with the particle size distribution should be explicitly included in the calibration process and they have to be determined prior to other parameters.

### 3.4 Validation of DEM models for segregation

The parameters obtained through calibration must be independent of the application (Coetzee, 2016). Therefore, once the model is calibrated, it should be capable of accurately reproducing other experiments. In order to prove this, the results of the DEM simulation have to be compared with either experimental tests, analytical or “well-established” numerical results related to segregation which are available in the literature. If a “good agreement” is observed, the model is validated. Regardless of the above-mentioned approaches being adopted for determining the DEM parameters, the studies in groups II, III and IV of **Table 1** (except for parametric studies in group I) at-

tempted to validate their DEM model for segregation. The validation techniques found in the literature overview of **Table 1** can be classified into two main categories as illustrated in **Table 6**: (1) using other research results as the benchmark and (2) using first-hand experimental results.

#### 3.4.1 Validation using other work’s results

In this approach, existing experimental, mathematical or numerical (i.e., DEM) results on segregation are used to validate the DEM model. Although adopting this approach facilitates the process of developing a DEM model, it suffers from several drawbacks. Firstly, some of these references have not particularly investigated the local behaviour (i.e., segregation) of granular materials and as a result, even in the case of an acceptable agreement, one cannot make sure the DEM model is valid for segregation. Secondly, in some cases, the size distribution of the DEM model differs from the source study against which the model has been validated. For example, Zhao et al. (2018) compared the results of the model for mono-sized particles and used the same model for modelling the segregation behaviour of granular materials with log-normal size distribution. However, according to Coetzee (2017), if particle size in the model changes, the model parameters must be recalibrated, i.e., the previous parameters’ values are not valid anymore. Thirdly, some studies employed a different setup in DEM than the experiment in the benchmark, which might significantly affect the simulation results. For instance, Wu et al. (2013) simulated a virtual factory instead of a conveyor belt in the original study (Kajiwara et al., 1988). While simplifying real-life scenarios is a common practice among researchers, it’s crucial to ensure that the velocity field is accurately mimicked, as it has a significant impact on segregation.

All in all, the approach of using other work’s results to validate the DEM model can have serious shortcomings. In other words, the model can be validated in this way only if all the details are accurately documented. This is often challenging since some data may have been omitted due to confidentiality. In addition, this approach is limited to specific materials (e.g., glass beads, iron ores), because there is a shortage of experimental data on the segregation of various kinds of granular materials in the literature.

#### 3.4.2 Validation by conducting experiments

Unlike the above-mentioned category which relied on existing data in the literature, other studies have conducted experiments themselves and used first-hand experimental data to validate the DEM model. Two types of experiments have been carried out (cf. **Table 6**): the flow-related measurements of the granular materials, i.e., global/bulk behaviour, or segregation-related measurements, i.e., local behaviour.

Examples of the first type of experiment in which

**Table 6** Validation approaches of past DEM studies on segregation (cf. **Table 1** for the type of mixture in each study).

Approach for validation		Source		
Other work's results	Experimental	(Liao et al., 2023; Wu et al., 2013; T.F. Zhang et al., 2020; Zhang et al., 2018; Zhao et al., 2018; Zhao and Chew, 2020b)		
	DEM	(Kumar et al., 2020; Mandal and Khakhar, 2019; Mantravadi and Tan, 2020)		
	Mathematical	(Ketterhagen et al., 2008; Ketterhagen and Hancock, 2010; Yu and Saxén, 2013; Zhao and Chew, 2020a)		
First-hand experimental results	Flow-related (bulk behaviour)	The mass fraction of the whole particles discharged from the hopper	(Tao et al., 2013)	
		The velocity profile of particles using particle tracking velocimetry (PTV)	(Shirsath et al., 2015)	
		Angle of repose measured in practice	(Kou et al., 2015; Tian et al., 2022)	
		The discharge time of the particles from the hopper	(Xu et al., 2017; 2018b)	
		Burden profile	(Kou et al., 2013; Yu and Saxén, 2013)	
		Mass distribution of “all” particles in the radial direction in furnace throat	(Kou et al., 2013)	
		Laser grid (Gao et al., 2010) measurement of burden falling trajectories	(Zhang et al., 2014)	
		Bed height	(Li et al., 2019)	
	Segregation (local behaviour)	Invasive	Sampling spaces composed of 24 cuboid-shaped cells inside the hopper	(Combarros Garcia et al., 2016)
			The discontinuous start-stop sampling method (Standish and Kilic, 1985) has been mostly adopted	(Ketterhagen et al., 2007; Yu and Saxén, 2010; Z. Zhang et al., 2020)
			Including a number of sampling boxes at the bottom to capture the trajectory segregation of materials	(Bhattacharya and McCarthy, 2014; Mio et al., 2008b, 2009, 2010, 2012; Yu and Saxén, 2012)
			Heaps are divided into a number of sub-regions in the horizontal and/ or vertical direction	(Li et al., 2017; Mio et al., 2020; Qiu and Pabst, 2022; Terui et al., 2017; You et al., 2016)
			Using rotating sampling table with pie slicing configuration	(Cliff et al., 2021)
			Measuring mass flow rate of fine particles using Copley flowability tester BEP2 model	(Barik et al., 2023)
			Sampling in the horizontal and vertical direction of the sinter cooler	(Izard et al., 2021)
Non-invasive	Sampling box in QPM segregation tester	(Combarros et al., 2014)		
	Taking pictures and counting the number of different components	(Yu et al., 2018)		
	Colouring equal-sized components and using image analysis to analyse segregation	(Combarros et al., 2014)		
		Taking pictures and using image processing to measure the fraction of components	(Alizadeh et al., 2017; Wang et al., 2018)	

physical measurements related to global behaviour have been carried out are listed in **Table 6**. With respect to segregation, this approach fails to provide detailed spatial and

temporal or “local” information about segregation such as the fraction of different components. Although this approach can be adequately adopted to validate DEM models

for “flow behaviour” on the bulk level, it cannot necessarily prove the validity of the model for segregation. In other words, to validate the models for segregation, component fractions are required to obtain local information and assess segregation.

The second type of the studies relied on segregation-related measurements. As can be seen in **Table 6**, there are two main ways of measuring segregation, namely invasive and non-invasive methods (Huang and Kuo, 2014). Invasive methods for evaluating segregation simply involve taking a number of samples, separating the components in each sample and weighting each component to obtain its mass fraction. Several sampling methods have been adopted by researchers for different systems as listed in **Table 6**. Although all the mentioned invasive methods are relatively simple and can provide valuable information about the local composition of granular mixtures, they have a number of disadvantages. First and foremost, invasive methods disturb the original structure of the mixture which affects the accuracy of the measurement. Moreover, particles from locations other than the target points might be collected during sampling (Muzzio et al., 1997). And, as mentioned above, components in each sample must be separated to further calculate their fractions. This can be straightforward for components differing in size, however for multi-component mixtures with overlapping particle sizes, this can be challenging and time-consuming. Terui et al. (2017) successfully employed the gravity separation method to separate sinter and coke particles based on the density difference. However, besides being time-consuming, this method is not applicable to all types of materials.

The mentioned drawbacks of invasive methods pushed the search for non-invasive techniques as an alternative. Because they do not disturb the granular structure, these techniques have been increasingly employed in recent years, especially in the powder blending industry (Nadeem and Heindel, 2018). There are several comprehensive review papers in the literature explaining the pros and cons as well as the applications and limitations of these methods in detail (Asachi et al., 2018; Bowler et al., 2020; Huang and Kuo, 2014; Nadeem and Heindel, 2018). Because of the inherent limitation of those techniques, not all of them are applicable to the segregation analysis of any granular mixture. For instance, the electrical conductivity method,

electrical capacitance tomography (ECT), positron emission particle tracking (PEPT) and magnetic resonance imaging tomography (MRI) cannot be readily utilised to analyse the mixing and segregation of all multi-component mixtures (Asachi et al., 2018). This is because the electrical conductivity method and ECT work based on the noticeable difference in electrical conductivity and permittivity, respectively, which is not the case in all multi-component mixtures (Asachi et al., 2018; Shenoy et al., 2015). Also, a limited number of tracers is tracked in PEPT, which is not suitable to measure segregation, and in MRI, the component should be coated with oil to be detectable, which might significantly affect its flow behaviour (Stannarius, 2017). Other techniques such as Raman spectroscopy, near-infrared spectroscopy (NIR) and acoustic emissions which are feasible for multi-components, are conducted on very small samples (Bowler et al., 2020), which makes them unsuitable for coarser particles. Image analysis is another existing non-invasive method which has been widely used due to its simplicity and low cost. The main advantage of image analysis over other techniques is that it is applicable to multi-component mixtures. However, this method is limited to surface analysis, it requires a transparent vessel and the components must differ in colour (Asachi et al., 2018). This method has been successfully employed by a number of studies to provide experimental results for the calibration and validation of DEM models of segregation. Yu et al. (2018) took photos of the heap, divided the heap into sub-regions radially and counted the number of small and coarse particles in each region to analyse segregation. Adopting a more robust approach, Wang et al. (2018) and Alizadeh et al. (2017) employed image processing techniques to measure local concentrations of mixture components at the surface of the heap. To be fully consistent, they used the same approach in DEM by taking snapshots of the granular system and applying image processing (see **Fig. 4**).

In conclusion, all the methods being adopted to validate DEM models come with a set of advantages and disadvantages. Although the use of existing results in the literature facilitates the validation, it is often difficult to precisely replicate the experimental setup and sometimes, the other study has not itself been validated. Additionally, utilising existing results is confined to a few materials which have

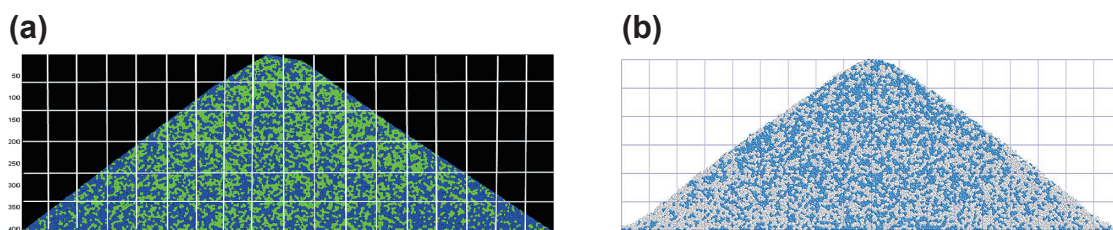


**Fig. 4** An example of using image analysis to measure segregation in (a) experiments and (b) DEM. Reproduced with permission from Ref. (Alizadeh et al., 2017). Copyright 2017, Elsevier.

already been investigated. To overcome these obstacles, carrying out experiments and using first-hand results would be beneficial. However, it should be noted that the experimental measurements should provide detailed spatial information for segregation on a local level supplemented by global level or bulk behaviour such as mass flow rate. The segregation-related measurements can be performed using either invasive or non-invasive methods. Image analysis as a non-invasive method is considered superior to invasive techniques since it not only maintains the structure of the granular materials but also is applicable to multi-component mixtures, provided that the components differ in colour.

#### 4. Results of DEM-based studies on segregation

The work we presented in Table 1 in the previous section will be elaborated in detail here. We gather and analyse the findings of those studies on how segregation is affected by adjusting material properties, system configurations and operational parameters.

##### 4.1 Material properties

Generally, any difference between the particles of a particulate system can cause segregation. For free-flowing granular materials, it has been proven that particle size, density and shape affect segregation more than other factors such as surface roughness and elasticity (Tang and Puri, 2004). The studies listed in Table 1 are analysed and the effect of these factors are presented in the following paragraphs. To systematically discuss the results in the literature, we present Fig. 5 which illustrates the possible combinations of different particle properties and Table 7 which shows the relevant subsection addressing the corresponding type of mixture.

###### 4.1.1 Particle size

Particle size is unequivocally the most influential property contributing to segregation among the other particle properties (Williams, 1976). This is why numerous research studies have been dedicated to gaining a full under-

standing of the effect of particle size and especially particle size distribution (PSD) on segregation.

In the case of binary-sized mixtures, i.e., mixtures in the form of  $1C[(2S/1Sh)]$ , the effect of size distribution can be investigated by varying either the size ratio or the mass fraction of the components. It is generally accepted that a larger size ratio leads to more pronounced segregation (Bridgwater, 1994). Fig. 6 shows the investigated ranges of size ratio in the DEM-based studies of binary-sized free-flowing mixtures in various systems. For hoppers and in one of the earliest attempts to study segregation using DEM, Ketterhagen et al. (2007) concluded that the extent of segregation significantly increases for size ratios greater than 1.9. Using the velocity difference between small and large particles as an indicator of percolation, T.F. Zhang et al. (2020) investigated the segregation during conical hopper discharging and found that in their case, percolation was not dominant for size ratios smaller than 6.0 (i.e., corresponding to the velocity difference of 0.07 mm/s). Z. Zhang et al. (2020) observed that the percolation which occurred during the discharge of a wedge-shaped hopper near the wall and the bottom of the hopper was eliminated

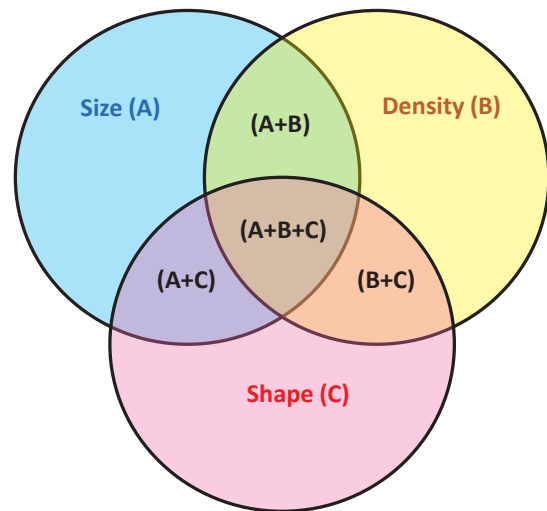


Fig. 5 Different possible combinations of particle properties.

Table 7 Corresponding subsection for different types of mixtures.

Section	Type of mixture		
	Symbol	Notation	
4.1.1 Particle size	A	$1C[(iS/1Sh)]$	$i = 2, 3, \dots, M, P$
4.1.2 Particle density	B	$nC[(1S/1Sh) + \dots + (1S/1Sh)]$	$n = 2, 3, \text{etc.}$
4.1.3 Particle shape	C	$1C[(1S/jSh)]$	$j = 2, 3, \text{etc.}$
4.1.4 Combinations of particle size, density and shape	(A+B)	$nC[(i_1S/1Sh) + \dots + (i_nS/1Sh)]$	$n = 2, 3, \text{etc.} \ \& \ i = 2, 3, \dots, M, P$
	(A+C)	$1C[(iS/jSh)]$	$i = 2, 3, \dots, M, P \ \& \ j = 2, 3, \text{etc.}$
	(B+C)	$nC[(1S/j_1Sh) + \dots + (1S/j_nSh)]$	$n = 2, 3, \text{etc.} \ \& \ j = 2, 3, \text{etc.}$
	(A+B+C)	$nC[(i_1S/j_1Sh) + \dots + (i_nS/j_nSh)]$	$n = 2, 3, \text{etc.} \ \& \ j = 2, 3, \text{etc.}$

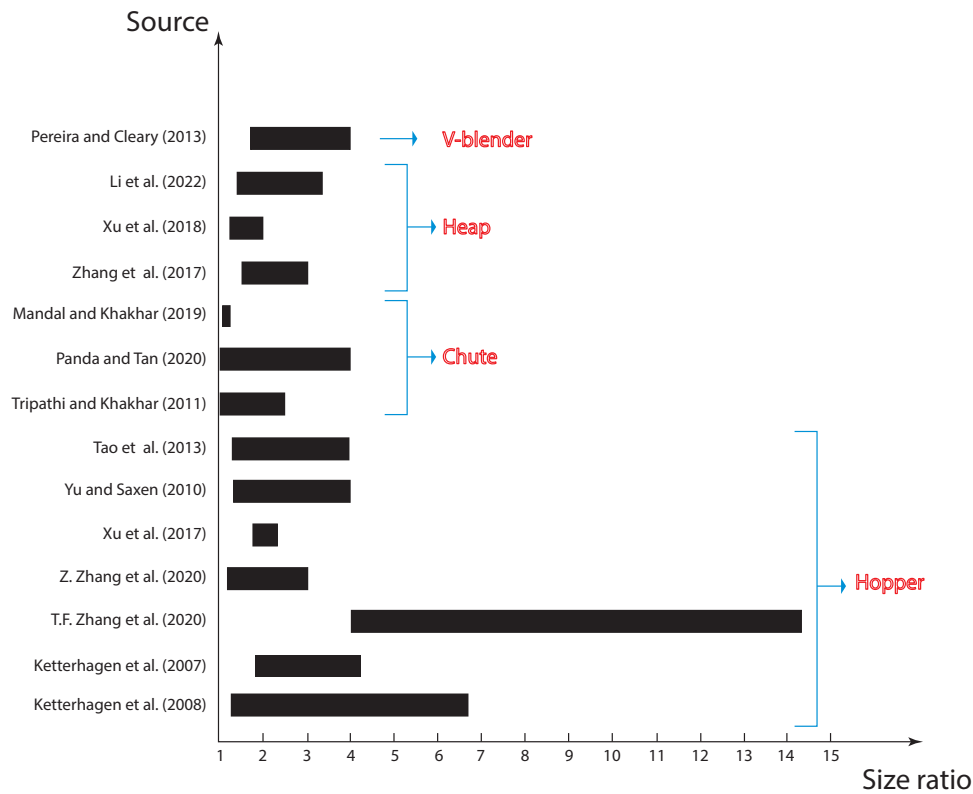


Fig. 6 Size ratio ranges in the past DEM studies on segregation.

for a size ratio lower than 1.2. Varying size ratios from 1.3 to 4.0, Yu and Saxén (2010) observed significant segregation even for the minimum ratio of 1.3. Unlike these studies, Ketterhagen et al. (2008) found that in the case of the hopper bottom wall angle of  $15^\circ$  (as opposed to  $90^\circ$ ), no considerable segregation was observed for all size ratios tested.

In addition to hoppers, several studies have examined the effect of size ratio on segregation in other systems such as inclined planes, chutes, the throat of the blast furnace and V-blender. In their work on the segregation of binary mixtures down an inclined plane, Tripathi and Khakhar (2011) found that varying size ratio does not affect the extent of segregation. In the case of a chute, Panda and Tan (2020a) observed that although the stream-wise, cross-stream and vertical velocities all increase with increasing size ratio, the degree of segregation did not increase significantly in the stream-wise direction. Li et al. (2022) studied the particle segregation in the throat of the blast furnace. For this, they charged a layer of binary-sized cokes followed by a layer of binary-sized ore particles. Varying the size ratio equally for coke and ore particles, they observed that larger size ratios result in a more segregated state, which was more evident for the coke mixture. In their study on the de-mixing of binary-sized mixtures during discharge from a V-blender, Pereira and Cleary (2013) observed that the segregation extent becomes significant for large size ratios, i.e., 3 and 4.

Apart from the particle size ratio, the mass fraction of fine particles has been proven to have a significant impact on segregation (Tang and Puri, 2004). Artega and Tüzün (1990) proposed a model for binary-sized mixtures to determine the fine mass fraction ( $x_f$ ) for which segregation via percolation becomes feasible during hopper discharge. They claimed that percolation no longer occurs when the surface area of the large spheres is completely covered by small spheres, implying that percolation only occurs if the mass fraction of finer particles is lower than the limiting value defined as  $x_{L,crit} = [4/(4 + \phi_R)]$ , where  $\phi_R$  is the size ratio. This model is applicable to free-flowing materials of approximately spherical shape and is independent of the hopper geometry. While the findings of Ketterhagen et al. (2008) and Z. Zhang et al. (2020) are in accordance with Artega and Tüzün's model, Xu et al. (2017) observed segregation for mass fractions higher than the above-mentioned  $x_{L,crit}$ . Nevertheless, all of these studies agree that increasing the fine mass fraction decreases segregation (Barik et al., 2023; Ketterhagen et al., 2008; Tian et al., 2022; Xu et al., 2017; Zhang et al., 2018; Z. Zhang et al., 2020).

While in most of the DEM studies a limited number of particle sizes has been used, Zhao et al. (2018) and Kumar et al. (2020) used a continuous distribution of particle size, i.e. poly-sized mixtures with the general form of  $1C[(PS/1Sh)]$ . Zhao et al. (2018) studied the discharge of mixtures with a log-normal size distribution from a conical

hopper. As shown in Fig. 7, they examined the effect of the width of size distribution, defined as the ratio of standard deviation to mean diameter ( $\sigma/\mu$ ) on segregation and concluded that the higher the width, the greater the size segregation will be. This agrees with observations on the impact of size ratio on the segregation of binary-sized mixtures, as the size ratio in binary-sized mixtures is essentially the same as the width of size distribution in poly-sized mixtures.

In another study, Kumar et al. (2020) studied the discharge from a hopper of mixtures with the Rosin-Rammler size distribution as follows:

$$R = 1 - \exp\left[-\left(\frac{x}{x'}\right)^n\right] \quad (2)$$

with size distribution's width ( $n$ ) and location parameters ( $x'$ ). It was found that the width has more impact on the segregation than location parameters. Moreover, they conducted a comparative analysis between the log-normal and Rosin-Rammler particle size distribution (PSD) with the same width and observed that the latter showed a higher segregation extent. They also reported that the extent of segregation is increased with more fine particles which contradicts the observations in past studies on the segregation of binary-sized mixtures (Ketterhagen et al., 2008; Xu et al., 2017; Zhang et al., 2018; Z. Zhang et al., 2020). This conflict may lie in the fact that comparing a continuous size distribution with a binary-sized mixture requires selection of the right cut-off size between fine and coarse particles, which is not always a trivial task.

To date, a large number of segregation-related studies focused on the effect of particle size and mass fraction in binary-sized mixtures. Generally, it has been found that reducing the size ratio as well as increasing the mass fraction of fine particles lessen segregation. With respect to the size ratio, however, there is no unanimous agreement either on the critical size ratio which promotes segregation or on

the effect of increasing the size ratio on segregation in general. Overall, there is no single limiting size ratio above which segregation happens. Also, there is no unanimous agreement on the effect of increasing the size ratio on segregation. The reason behind this is twofold. Firstly, apart from size ratio, other factors such as material properties (e.g., mass fraction), geometric, and operational parameters also play a crucial role in segregation phenomena. Secondly, percolation rate measurements in shear cells have shown that segregation can occur for all size ratios, and larger size ratios only serve to accelerate its occurrence (Bridgwater, 1994; Bridgwater et al., 1978; Tang and Puri, 2005). Similar to the size ratio, the effect of the mass ratio of fine particles on segregation is not consistent, leading to the conclusion that the results of one study cannot be applied to all cases since other factors (e.g., geometrical and operational parameters) play a key role as well.

#### 4.1.2 Particle density

The difference in particle density is another known factor to cause segregation. As mentioned in Section 2, the density of particles in a single material is assumed to be constant. Therefore, the difference in particle density is equivalent to having different materials. For instance, what is referred to as a “binary-density” mixture is basically a two-component mixture with the notation of  $2C[(1S/1Sh) + (1S/1Sh)]$ .

While a number of earliest experimental studies on the mixing and segregation of granular materials argued that particle density does not affect segregation considerably (Vallance and Savage, 2000; Williams, 1976), some others suggested that the difference in density should be taken into account in segregation analysis (Bridgwater et al., 1978; Drahun and Bridgwater, 1983; Khakhar et al., 1999). There has been, however, little systematic analysis of density-driven segregation in free-flowing granular materials using DEM. Seil et al. (2012) investigated the segregation of mixtures discharging from two hoppers. They observed that the heavier particles tend to gather in the centre areas and that the extent of segregation is linear to the density ratio. In another study on an inclined plane, Tripathi and Khakhar (2013) observed that heavy particles sink to near the base, and light particles form a layer close to the free surface with a mixed region in between, which was confirmed in other studies (Panda and Tan, 2020a; Wang et al., 2018, 2023). Furthermore, they showed that higher density ratios result in stronger segregation.

In conclusion, particle density has been shown to affect segregation to some extent. However, the significance of its effect compared to other factors such as the difference in particle size is unclear as yet. More effort on density-induced segregation in various systems is required to pave the way for developing DEM models for multi-component segregation.

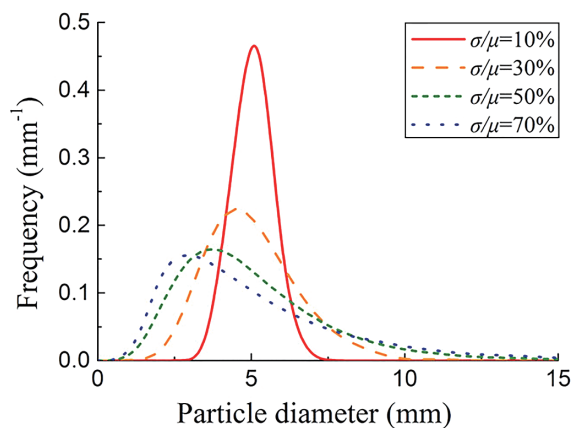


Fig. 7 Different log-normal size distributions. Reproduced with permission from Ref. (Zhao et al., 2018). Copyright 2017, John Wiley and Sons.

#### 4.1.3 Particle shape

Only a few of the studies found focused on modelling the effect of particle shape on the extent of segregation. These studies can be classified into two groups. The first group includes studies in which the mixtures are composed of two particle shapes to investigate shape-induced segregation. Using the multi-sphere approach, Mandal and Khakhar (2019) studied the flow of mixtures of spherical and non-spherical particles of the same volume down a rough inclined plane (cf. Fig. 8). They found that the geometric mean diameter (i.e.,  $d_g = \lambda^{1/3}d$ , where  $\lambda$  is the aspect ratio and  $d$  is the diameter of the constituent spheres) is a good representative of the effective size for irregularly shaped particles, and the extent of segregation of two species depends on the ratio of the geometric mean diameter of particles. Moreover, it was observed that at the steady state, the particles with a larger geometric mean diameter accumulate near the free surface.

Zhao and Chew (2020a) studied the flow behaviour of binary-shaped mixtures during discharge from a hopper. They modelled seven different particle shapes (a sphere, two ellipsoids, two cylinders, and two cuboids (as shown in Fig. 9), all with an aspect ratio between 0 and 2 and the same volume. Considering various combinations of these particle shapes, they observed that mixtures of cylinders and cuboids exhibited the least segregation and the ellipsoids mixed with cylinders were the most segregated mixtures.

Second, studies in which the segregation behaviour of different mixtures, each component composed of a particular shape, is analysed. Zhao and Chew (2020b) compared the discharging behaviour of mixtures with log-normal PSD composed of ellipsoids, cylinders or cuboids and observed that ellipsoids show a very similar segregation behaviour to spheres. The cuboids and ellipsoids exhibit the lowest and the highest segregation extent, respectively.

Concluding, very little attention has been paid to shape-induced segregation in DEM-based studies. Past studies have demonstrated that the difference in particle shape itself can induce segregation (Mandal and Khakhar,

2019; Zhao and Chew, 2020a). However, it is unclear how particle shape induces segregation and specifically, which shape characteristics are more significant for segregation. Therefore, further work needs to be done to shed light on shape-induced segregation. Challenging herein are the computational expense of irregularly shaped particles and the fact that particle shape is not independent of particle size. This is very important since if only the segregation induced by particle shape is of interest, the “effective” particle size should be the same to avoid misinterpretation (Shekhar et al., 2023). Therefore, we second that attempts should be made to establish the criteria for finding the “effective” size of non-spherical particles for segregation (Yu et al., 2020).

#### 4.1.4 Combinations of particle size, density and shape

While the preceding subsections were focused on studies examining variations in a single particle property (such as size, density, or shape), a limited number of research works investigated mixtures with multiple properties that vary simultaneously. To systematically discuss them, these studies are grouped below using the symbols in Fig. 5 and Table 7:

(A+B). Most of the studies varied the particle size and density at the same time. Two different scenarios can be distinguished: 1. a mixture of (small/heavy) and (large/light) particles, in which the percolation and buoyancy mechanisms work together, or, 2. a mixture composed of small/light and large/heavy particles where percolation and buoyancy mechanisms oppose each other. Fig. 10 illustrates these two scenarios. As can be seen in Fig. 10(a), in the first scenario, both percolation and buoyancy mechanisms act together and (small/heavy) particles sink into the mixture. However, in the second scenario as in Fig. 10(b), the dominant segregation mechanism is not known a priori and should be studied case by case. Past studies indicated that in the first scenario, reducing the size ratio and/or density ratio leads to less segregation and could be used as a way to suppress segregation (Terui et al., 2017; Xu et al., 2017, 2018a). For the second scenario, Ketterhagen et al.

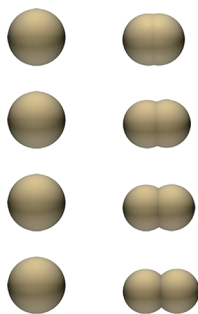


**Fig. 8** Different combinations of spherical and non-spherical particles. Reproduced with permission from Ref. (Mandal and Khakhar, 2019). Copyright 2019, AIP Publishing.

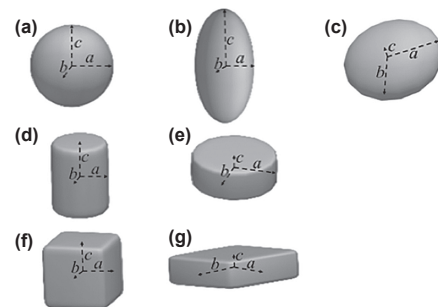


**Fig. 9** Different particle shapes modelled. Reproduced with permission from Ref. (Zhao and Chew, 2020a). Copyright 2020, John Wiley and Sons.

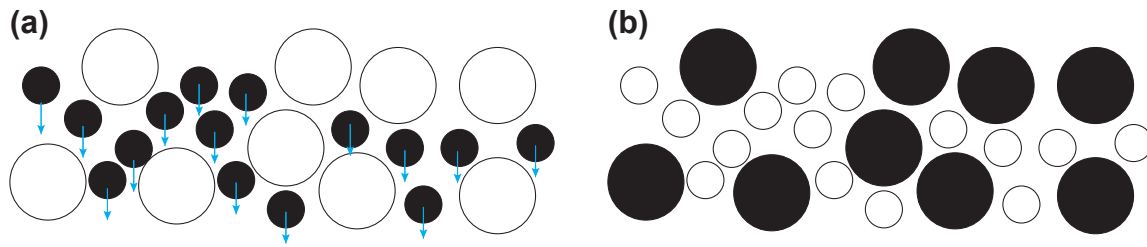


**Fig. 10** Two scenarios for particles differing in both size and density (solid black colour indicates heavier particles), **(a)** first scenario; a mixture of (small/heavy) and (large/light) particles, and **(b)** second scenario; a mixture of (small/light) and (large/heavy) particles.

(2008) varied the density ratio from 0.33 to 3.0 for a size ratio of 4.3, and no significant segregation was detected during discharge from a wedge-shaped hopper. Similarly, Tao et al. (2013) increased the density ratio from 0.5 to 2.0 for a mixture with a size ratio of 4.0 and observed that segregation was negligible.

**(A+C).** In attempts to explore the simultaneous effect of particle size and shape on segregation, several studies varied the particle shape of binary-sized mixtures, i.e. mixtures in the form of  $1C[(2S/2Sh)]$ . Mandal and Khakhar (2019) studied the flow of mixtures of non-spherical particles where the two particle types differ in both volume (i.e., size) and shape, and observed that the segregation extent increases for larger geometric mean diameter ratios. Tao et al. (2013) simulated binary-sized mixtures with different particle shapes including spherical, corn-shaped, cylindrical and ellipsoidal particles. It was observed that particle shape has a significant effect on the segregation extent with the most segregated system for ellipsoidal and the least for spherical particles.

**(A+B+C).** A few studies examined the segregation in mixtures differing in particle size, density and shape. Liao et al. (2023) investigated the segregation behaviour of lump ore and pellets that differed in size and density. To examine the impact of particle shape on segregation, they simulated three different shapes of lump ore particles, namely spheres, cylinders, and schistous particles and concluded that particle shape has a significant effect on segregation, with spheres showing the least amount of segregation. In the mixture of sinter and briquette, Kim et al. (2020) changed both the shape and mass ratio of the briquette and observed that while the shape had little effect on segregation, a mass ratio higher than 20 % led to significant segregation.

Despite previous efforts to investigate the influence of various material properties on segregation, there remains a significant knowledge gap. While the majority of natural and industrial mixtures are multi-component, i.e. **(A+B+C)** in **Table 7**, most studies have concentrated on binary or ternary-sized mixtures consisting of spheres. Therefore, a more comprehensive and rigorous approach towards material properties that takes various combinations of size, density and shape into account is required to accurately

predict segregation patterns and occurrences.

## 4.2 System configurations

In addition to the material properties, system parameters play a key role in the segregation phenomena occurring in particulate systems because they influence the motion of the particles. In gravity-driven handling processes, two main pieces of equipment can be distinguished: hopper/silo and chute/inclined surfaces. A review of these systems in the context of segregation is presented in the following paragraphs.

### 4.2.1 Hopper

Segregation during hopper discharge has been studied since the early '80s when most studies were experimental. Ketterhagen et al. (2007) were one of the first to model segregation during cylindrical hopper discharge using DEM in 2007. Since then, a number of DEM studies have investigated the influence of geometric properties on the extent of segregation by varying the outlet width, the slope of the bottom wall and the smoothness of the walls.

Two main flow regimes are distinguished during hopper discharge: mass flow, where the entire body of mass inside the hopper is in motion during discharge, and funnel flow (Jenike, 1967; Saleh et al., 2018; Schulze et al., 2008); funnel flow is less desirable as it imposes asymmetric pressure distribution and causes significant segregation which can be harmful to both hopper structural stability and particulate homogeneity (Saleh et al., 2018). The flow mode is mainly dependent on the bottom wall angle ( $\theta_c$ ) and wall friction angle ( $\phi_x$ ). Smoother and steeper walls (i.e., low  $\theta_c$ ) most likely induce a mass flow regime and are less likely to induce segregation. This was also confirmed in several DEM studies (Ketterhagen et al., 2009, 2008; Saleh et al., 2018; Yu and Saxén, 2010).

Several studies used DEM to gain a deeper insight into segregation during hopper discharge. T.F. Zhang et al. (2020) varied the angle of the hopper wall from  $15^\circ$  to  $90^\circ$  and observed that larger angles (i.e., flatter walls) lead to faster percolation of small particles, increasing their tendency to gather at side walls (cf. **Fig. 11(a)**). Similarly, Z. Zhang et al. (2020) showed that the increase in the hopper angle promotes segregation in the bottom regions (red

regions in Fig. 11(b)). However, they found that with larger angles, the percolation near the wall region decreases. This disagreement might be because of the different size ratio, wall condition (i.e. boundary walls in T.F. Zhang et al. (2020)), or a different method of assessing segregation (cf. Section 3.2). Also, it is remarkable that in T.F. Zhang et al. (2020), the hopper outlet size of  $3d_1$  (where  $d_1$  is the diameter of the large particles) is used, which does not satisfy fundamental hopper design principles (Schulze et al., 2008) and can affect the segregation results.

Stating that the bottom angle of the hopper is a decisive factor in the flow mode, Huang et al. (2022) proposed an optimised design which increases the mass flow zone and as a result, achieves less size segregation (cf. Fig. 12).

In addition to the hopper wall angle, the outlet size can

also affect segregation during hopper discharge. Ketterhagen et al. (2008) found that the increase in outlet width reduces the segregation of mixtures discharging from wedge-shaped hoppers. Although Z. Zhang et al. (2020) confirmed that the percolation in the bottom part of the hopper reduces in the case of a bigger outlet, a higher segregation degree near hopper walls was observed which can be related to wall effects. Taking the effect of both the hopper outlet and wall angle into account, Ketterhagen et al. (2008) claimed that segregation conditions remain the same for hoppers with the same aspect ratio of hopper height to hopper width.

To investigate the effect of flow-correcting inserts, Cliff et al. (2021) compared the segregation behaviour of binary-sized mixtures during discharge from a hopper with

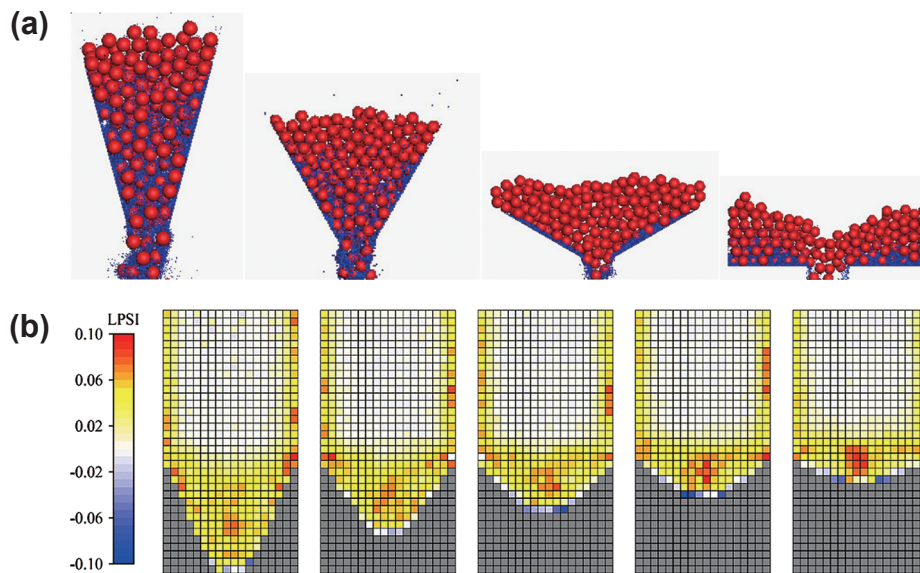


**Fig. 11** The effect of hopper wall angle on size segregation in two studies: (a) Reproduced with permission from Ref. (T.F. Zhang et al., 2020). Copyright 2020, Elsevier. and (b) Reproduced from Ref. Z. Zhang et al. (2020), used under Creative Commons CC-BY-NC-ND License.

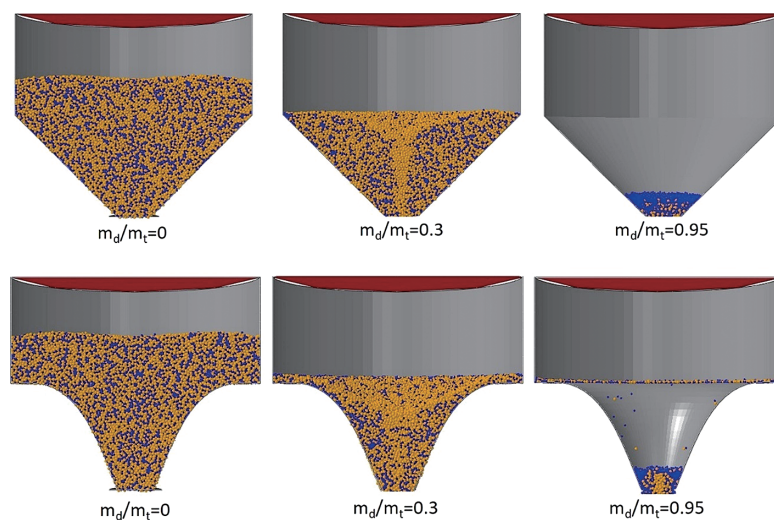


**Fig. 12** The effect of different hopper design on segregation during hopper discharge at different discharging fractions ( $m_d/m_t$ ). Reproduced with permission from Ref. (Huang et al., 2022). Copyright 2022, Elsevier.

and without an insert (cf. **Fig. 13(a)**). They stated that in the case of a hopper with an insert, lower velocity gradients at the free surface lead to less segregation (cf. **Fig. 13(b)**).

While most of the works mentioned above studied concentric hoppers, Ketterhagen and Hancock (2010) compared the segregation of binary-sized mixtures in eccentric and concentric hoppers (cf. **Fig. 14(a)**). They found that while the eccentric hopper had slightly less segregation, the segregation profiles around the outlet were completely different (cf. **Fig. 14(b)**). Additionally, they modified the design of the eccentric hopper, resulting in improved segregation.

In conclusion, designing for mass flow is beneficial to avoid size segregation during hopper discharge. This can be achieved by steeper and smoother walls. However, several studies observed insignificant effects of these factors on segregation. The reason for the conflict between these studies is that besides geometric parameters, material properties and operational parameters can influence particle velocities and segregation. This makes it challenging to compare the findings of different studies and arrive at a definitive conclusion. Therefore, a more robust approach is

needed to investigate the simultaneous effect of different geometric factors on segregation and its dependence on material properties. Moreover, the work found evaluated only single-component mixtures, and the effect of geometric design parameters in the case of multi-component segregation is missing.

#### 4.2.2 Chutes

Chutes are often used to transfer materials from one piece of equipment to another. They can have different cross-sectional shapes (e.g., semicircular, rectangular), lengths, curvatures and wall roughness. While the chute angle may be regarded as a system configuration parameter in certain cases, e.g., transfer chutes, it is considered an operational parameter in dynamic systems such as blast furnaces. Therefore, we will be discussing the chute angle later in **Section 4.3.2** of this paper.

Segregation can occur simultaneously in three directions: in the direction of the flow (longitudinal/stream-wise segregation), from the chute to the free surface (vertical/normal segregation) and from one side wall to the other (horizontal/cross-stream-wise segregation). During chute

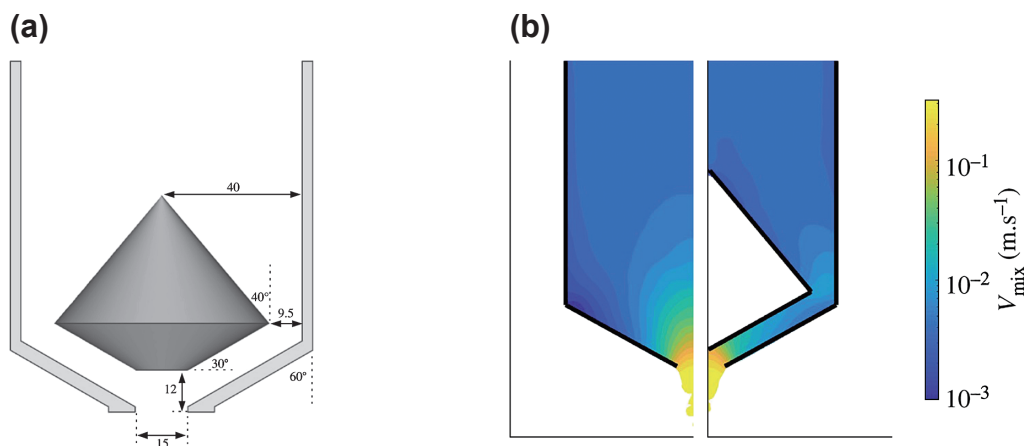


**Fig. 13** (a) The cross-sectional view of the hopper with insert, (b) Difference in the velocity gradient between the hopper with (right) and without (left) insert. Reproduced with permission from Ref. (Cliff et al., 2021). Copyright 2021, The Royal Society.

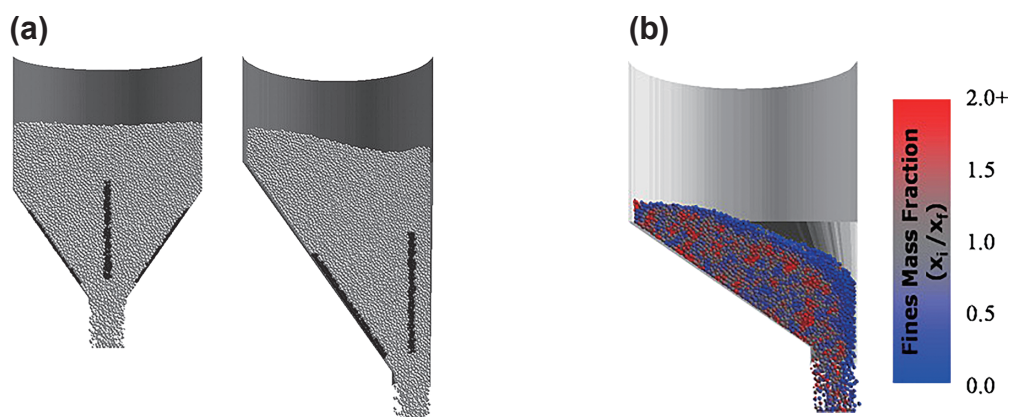


**Fig. 14** (a) Concentric and eccentric hopper, and (b) Segregation profile in the eccentric hopper. Reproduced with permission from Ref. (Ketterhagen and Hancock, 2010). Copyright 2010, Elsevier.

flow, segregation can happen in two stages. Firstly when the material is inside the chute, gravitational forces, centrifugal and Coriolis forces, inter-particle friction and particle-wall friction forces act on the particles (Zhang et al., 2014). Mio et al. (2008b) found that particles segregate inside the chute with smaller particles at the bottom wall of the chute and larger ones on top. In the second stage, the material leaves the chute and trajectory segregation causes larger particles to travel further (Mio et al., 2008b). The effect of chute-related geometric parameters on segregation was researched by employing either a simple inclined plane (Zhao et al., 2022) (to minimise the effect of side walls) or a real 3D chute (Panda and Tan, 2020a).

With respect to the effect of the cross-sectional shape of the chute, Kou et al. (2019) investigated the effect of three different shapes, namely semi-circular, trapezoid, and rectangular on the segregation of ferrous burden (i.e., pellet, sinter and lump ore) forming a heap in the blast furnace throat. They found that the chute cross-sectional shape significantly affects the radial size distribution of materials and the effect is intensified with larger chute angles and higher rotating speeds. Moreover, unlike trapezoid and rectangular chutes, the semi-circular chute was reported to maintain a uniform radial size distribution regardless of the chute angle and rotating speed. Panda and Tan (2020a; 2020b) focused on the segregation inside the chute and compared the segregation between rectangular and semi-circular chutes. It was observed that the rectangular channel resulted in slightly higher segregation in the stream-wise direction, while there were barely any differences in cross-stream and vertical directions.

In terms of the impact of chute length, the observations revealed that since segregation occurs within the chute, an increase in the chute length leads to a greater extent of segregation (Bhattacharya and McCarthy, 2014; Kou et al., 2013; Yu and Saxén, 2012; Zhang et al., 2014). Bhattacharya and McCarthy (2014) determined the critical chute length for trajectory segregation of ternary-sized mixtures discharging from a hopper on to the chute, using both theoretical equations and simulations which yielded 4.0 and 5.4 m, respectively. They claimed that with other parameters fixed, there is significant segregation in the sampling boxes located under the chute for the chute longer than the critical length. For the radial segregation of multi-component mixtures of sinter, pellet and ore, Hong et al. (2021) observed that the effect of chute length is negligible.

Mantravadi and Tan (2020) examined the effect of bend angle (i.e. curvature) in periodic flow inversions (see Fig. 15)—an idea initially introduced by Shi et al. (2007)—on reducing the size segregation of binary-sized mixtures and observed that a bend angle between 120 and 150 degrees leads to the minimum extent of segregation.

Zhou et al. (2016) varied the wall roughness by using the wall friction coefficient and found that a higher base rough-

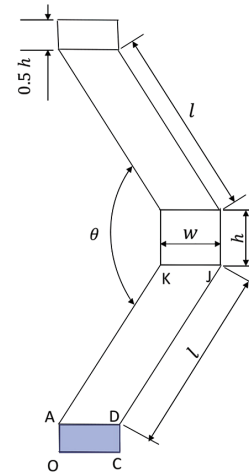


**Fig. 15** The periodic flow inversion with a bend angle of  $\theta$ . Reproduced with permission from Ref. (Mantravadi and Tan, 2020). Copyright 2020, Elsevier.

ness significantly accelerates segregation. However, in the case that base friction was larger than inter-particle friction, no effect on the flow regime and segregation was observed. Shirsath et al. (2015) studied the effect of chute wall roughness on the segregation of binary-density mixtures, i.e.,  $2C[(1S/1Sh) + (1S/1Sh)]$ . They implemented the roughness artificially by modelling a number of particles at chute walls, attributing the ratio of the diameter between surface particles and flowing particles (ranging from 0.5 to 2.0) to the degree of roughness. They reported that wall roughness has a considerable effect on segregation as it is negligible for the smooth (but frictional) chute wall. While it was observed that the degree of segregation increases with wall roughness, this increase plateaus when the diameter of wall particles exceeds the flowing particle size. However, it is unclear to what extent the method of modelling wall roughness in this work is representative for roughness at micro scale.

Concluding, the geometric aspects of chutes including cross-section shape, length, curvature and wall roughness can significantly influence segregation. Generally, it has been found that longer chutes with rougher walls promote segregation.

### 4.3 Operational parameters

Besides the material properties and system configurations discussed above, operational parameters are also among the influencing factors on segregation. In order to gain a deeper insight, related studies are reviewed in the following subsections under different categories based on the system type, namely hopper, chute and other systems.

#### 4.3.1 Hopper filling operations

Various hopper-related operational parameters, including filling method, filling angle, and filling position have been studied in the past. Several studies investigated the

influence of various hopper filling methods, i.e., different components/sizes being charged in separate layers or in a pre-mixed state, on the segregation after hopper discharge (Chibwe et al., 2020; Ketterhagen et al., 2008, 2007; Mio et al., 2010; Yu and Saxén, 2010). Although Ketterhagen et al. (2008), Yu and Saxén (2010) and Chibwe et al. (2020) used slightly different setups and filling patterns, their conclusion was that the initial filling method significantly affects the segregation.

Apart from the filling method, the filling position was found to significantly influence segregation. Wu et al. (2013) investigated the effect of burden apex (i.e., the highest point on the hill formed when materials are charged into the hopper) on the segregation during hopper charging and discharging. It was found that the burden apex mostly influences the particle size distribution during charging but has little effect during discharging. In the case of a Paul-Wurth hopper, Zhang et al. (2021) also observed that the filling position has a significant effect on the segregation and there was strong segregation in the case of the right and left filling positions (cf. Fig. 16(a)). Moreover, they observed that a filling angle closer to the vertical position (cf. Fig. 16(b))

and a larger charging outlet (cf. Fig. 16(c)) reduced the extent of segregation.

Cliff et al. (2021) showed that a continuous filling operation, as opposed to batch processing, significantly reduces the amount of segregation because segregation mostly occurs in the last 25 % of hopper discharge.

Concluding, the filling method, filling position and filling angle significantly affect segregation downstream (i.e., during hopper discharge). This means that all the handling steps should be accurately modelled in order to achieve a reliable assessment of segregation.

#### 4.3.2 Chute operations

With respect to chute-related operational parameters, several studies have investigated the effect of chute angle ( $\theta$ ) (Jing et al., 2015; Kou et al., 2019, 2018, 2013; Mio et al., 2009; Nakano et al., 2012; Tripathi and Khakhar, 2011; Xu et al., 2018b; You et al., 2016; Zhang et al., 2014), tilting direction (Terui et al., 2017), rotating speed ( $\omega$ ) (Kou et al., 2019, 2013; You et al., 2016), fill level (Izard et al., 2021; Panda and Tan, 2020a), the number of chute rotations (Mio et al., 2012) and installation of a damper (Mio et al.,

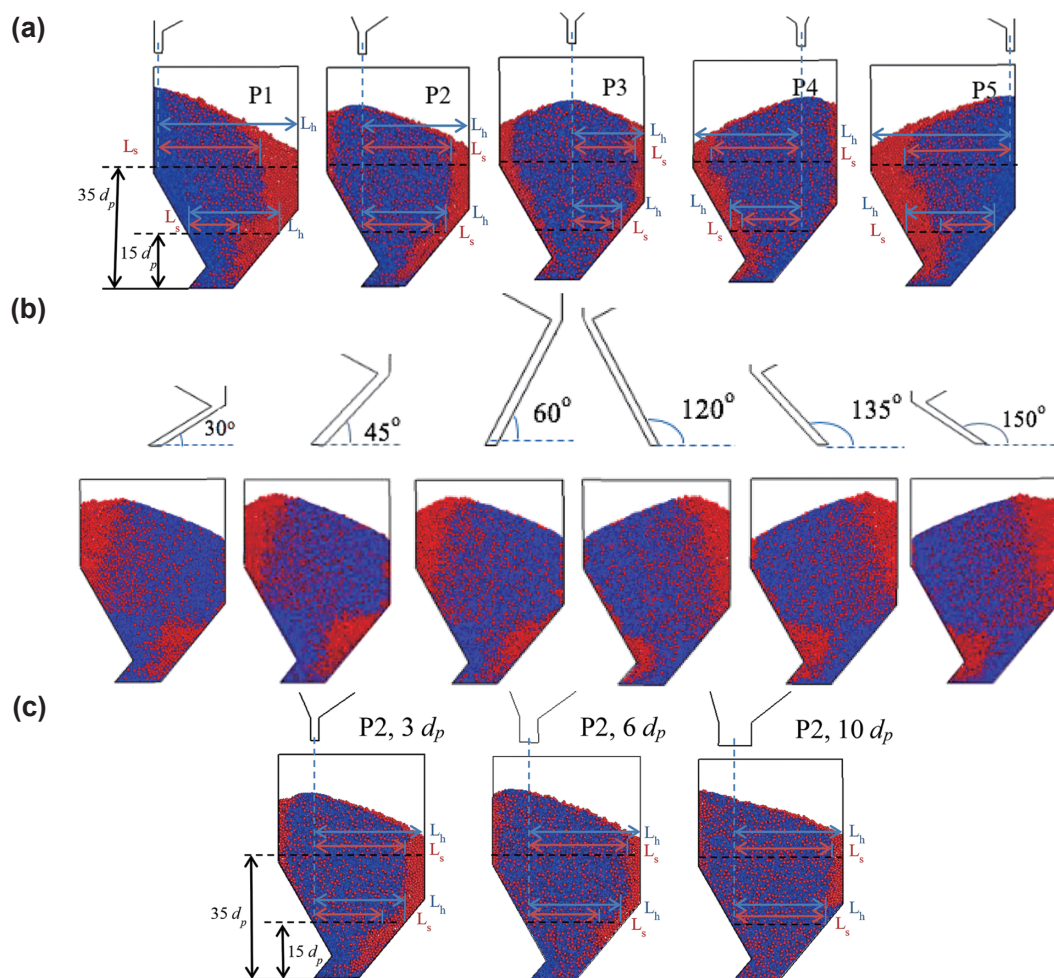


**Fig. 16** The effect of (a) filling position, (b) filling angle and (c) hopper outlet on segregation during hopper charging. Reproduced with permission from Ref. (Zhang et al., 2021). Copyright 2021, Elsevier.

2008b). Some of the parameters are schematically illustrated in Fig. 17.

It should be noted that in a rotating chute, particles are subjected not only to gravitational forces but also to Coriolis and centrifugal forces (Shirsath et al., 2015). The relative impact of inertial and Coriolis forces is quantified by the Rossby number (Eqn. (3)):

$$Ro = \frac{v_a}{2\omega L \cos \theta} \quad (3)$$

where  $v_a$ ,  $\omega$ ,  $L$ , and  $\theta$  denote the flow velocity, chute rotation rate, chute length and chute angle, respectively. In the case of  $Ro \gg 1$ , the effect of the rotation rate can be neglected. For instance, Shirsath et al. (2015) varied the chute rotation rate from 4 to 16 rpm and observed  $Ro$  larger than 1, concluding that the flow was gravity driven. Also, the Froude number (Eqn. (4)) can be used to quantify the relative significance of the centrifugal force compared to the gravitational force (Shirsath et al., 2015):

$$Fr = \frac{\omega^2 L \cos \theta}{g} \quad (4)$$

In the case of  $Fr \ll 1$ , the gravitational force is dominant, preventing the particles from escaping out of the chute.

The chute angle is an important flow control parameter as it is used to increase or decrease the flow velocity. Past DEM studies have investigated the effect of chute angle on the segregation occurring either inside the chute or when particles flow out and form a heap. Regarding the segregation happening inside the chute, Tripathi and Khakhar (2011) observed that the shear rate and extent of segregation in a vertical direction increased with a lower angle. Similarly, Jing et al. (2015) found that segregation occurs faster as the angle decreases, which was expected since the rate of acceleration increases as the chute is steeper. However, the final (converged) segregation degree was similar

for different chute angles and, surprisingly, the converged state was reached at approximately the same time for different angles.

For segregation occurring after discharging from chutes, several studies have found that reducing the chute angle intensifies the segregation in different systems, namely blast furnace throat (Kou et al., 2019; Mio et al., 2009; Xu et al., 2018b; Zhang et al., 2014), feed bed of sintering machine (Nakano et al., 2012), COREX melter gasifier (Kou et al., 2015, 2013; You et al., 2016). However, Zhang et al. (2014) varied the chute angle from 21° to 37° and observed that the radial segregation index (RSI) would not necessarily decrease (cf. Fig. 18). Also, Kou et al. (2013) observed that increasing the chute angle from 10° to 30° first leads to a decrease of segregation of large particles and then to an increase.

In modern blast furnaces equipped with the Paul-Wurth Bell-Less Top® charging system, as well as in the COREX process, a rotating chute is used to distribute materials in the circumferential directions of the furnace throat (Cameron et al., 2019; Kou et al., 2013). In addition to the previously discussed chute angle, other operational parameters such as the rotating speed, tilting direction (i.e. changing the angle from low to high or vice versa as shown in Fig. 17), and the number of rotations have been studied with respect to segregation. Terui et al. (2017) modelled a mixture of coke and sinter and two types of tilting directions, namely conventional tilting (i.e., from wall to centre direction) and reverse tilting (i.e., from centre to the wall direction). They found that with reverse tilting, coke particles are less segregated as shown in Fig. 19. The rotating speed of the chute was found to have a negligible effect on segregation compared to the chute angle (Kou et al., 2019, 2013; You et al., 2016). Mio et al. (2012) observed that an increase in the number of chute rotations intensifies segregation, leading to a larger mean particle size near the

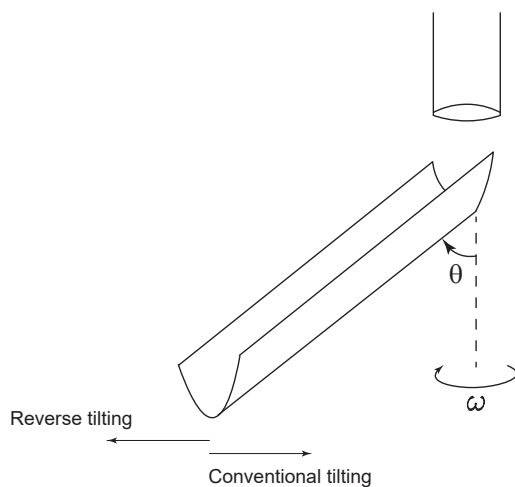


Fig. 17 Schematic view of a rotating chute and related operational parameters: chute angle ( $\theta$ ), rotating speed ( $\omega$ ).

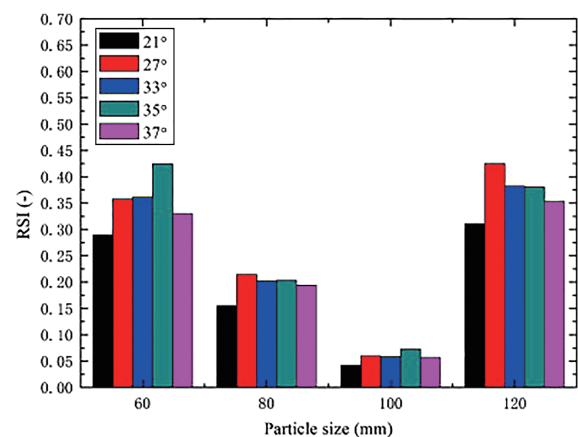


Fig. 18 Change in radial segregation index (RSI) with different chute angle. Reproduced with permission from Ref. (Zhang et al., 2014). Copyright 2014, Elsevier.

centre of the blast furnace.

The volume (or mass) flow rate through a chute is another operational parameter which is generally varied on an on-demand basis. For a given chute design, increasing/decreasing the flow rate results in a higher/lower fill level of the chute. Panda and Tan (2020a) found that the increase in the fill level causes the small and large particles to move together, i.e., decreases the velocity difference, resulting in lower segregation in the cross-stream and vertical directions of the chute. Although it was observed that the fill level does not affect velocities in a stream-wise direction, segregation was decreased because of less available space for percolation due to denser packing. In a study on sinter cooler charging systems, Izard et al. (2021) investigated the effect of the fill level of the chute (i.e. 20 %, 50 % and 90 %) on the segregation pattern in the trolleys and found that while a filling ratio smaller than 50 % imposes an increasing size heterogeneity in the trolley, no change in the segregation pattern was observed for a filling ratio larger than 50 %.

In conclusion, the operational parameters for operating moving chutes including chute angle, tilting direction, rotating speed and fill level, affect the segregation to some extent. Based on the studies reviewed here, it appears that chute angle and fill level may be more significant than the other parameters. However, further research is needed to confirm this hypothesis and to fully understand the complex nature of segregation in granular mixtures discharging from moving chutes. Nevertheless, all the parameters have the potential to be adjusted with the purpose of reducing or

controlling segregation.

#### 4.3.3 Other systems

In addition to hoppers and chutes, other operation-related factors have been investigated in the context of the gravity-driven segregation of cohesionless materials. This includes the falling height in the stockpile (Kou et al., 2013; Zhang et al., 2017), the method of “discharge” from a v-blender (which is essentially a gravity-driven flow) (Pereira and Cleary, 2013), the bottom base shape of the COREX furnace (cf. Fig. 20) (Kou et al., 2018) and feed rate as well as rill plate angle in an iron ore sinter strand (Li et al., 2019). Hence, in every industrial system, there are several operational parameters that can affect segregation. Detecting these parameters and studying their effect utilising DEM can pave the way to optimise the industrial processes with respect to segregation. This is highly advantageous because, in industrial applications, it is not always possible to control segregation by modifying material properties and system configurations.

### 5. Conclusion

This review paper presents an overview of the state of the art in the DEM modelling of the segregation behaviour of complex multi-component mixtures in applications involving the gravity-driven flow of dry, cohesionless granular materials. First of all, a novel scientific notation has been introduced to ensure consistency and accurately describe different types of mixtures. The main findings of this review can be summarised as follows:

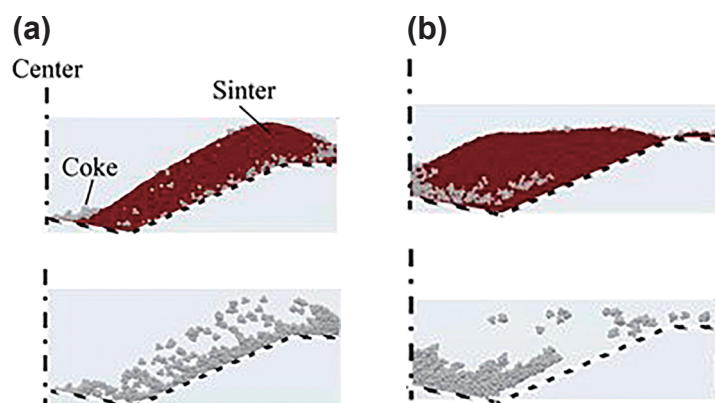


**Fig. 19** Cross-sectional view of the radial distribution of a coke-sinter mixture for (a) reverse tilting and (b) conventional tilting. Reproduced with permission from Ref. (Terui et al., 2017), used under Creative Commons CC-BY-NC-ND License.

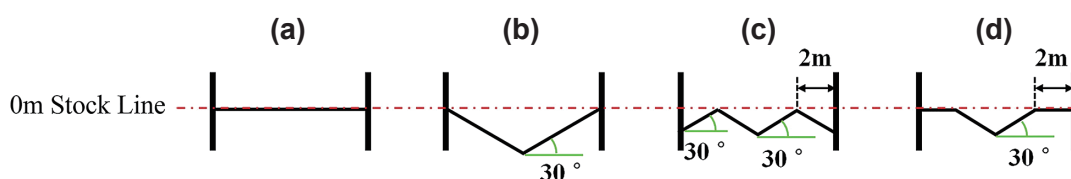


**Fig. 20** Different bottom base shape of the COREX furnace. Reproduced with permission from Ref. (Kou et al., 2018). Copyright 2018, Elsevier.

- Although most mixtures existing in nature and industrial settings are considered multi-component (i.e., they contain particles differing simultaneously in size, density and shape), relatively few studies have investigated the segregation behaviour of such mixtures.
- Despite the fact that calibration is an essential part of developing a reliable DEM model, most of the past studies have omitted it. This is especially true when it comes to models of multi-component mixtures. For instance, the effect of interaction parameters between components has not yet been studied in detail. Furthermore, it is not clear whether calibrated parameter values obtained for a certain mixture composition are applicable to other compositions as well.
- The effect of size distribution and particle shape on segregation has not yet been fully understood. Considering the fact that including small particles and irregular particle shapes in the model increases computational time considerably, the effect of approximating real-world mixtures with a finite number of particle sizes and spherical particles should be comprehensively studied.
- When quantifying segregation experimentally, non-invasive techniques such as image analysis are generally more suitable than conventional invasive methods (i.e., sampling and weighing), since non-invasive techniques do not disturb the mixture structure and are applicable to mixtures differing in both size and density.
- Results of past DEM studies on segregation show that the effects of different parameters influencing segregation, i.e., material properties, system configurations and operational parameters, should be considered together since they are highly intertwined.
- Compared to material properties and system configurations, operational parameters are relatively easier to change. Hence, to reduce and control segregation in industrial applications, operational parameters are preferential.

## Acknowledgements

This research was carried out under project number T18019 in the framework of the Research Program of the Materials innovation institute (M2i) ([www.m2i.nl](http://www.m2i.nl)) supported by the Dutch government. Also, this work was carried out as part of the “Industrial Dense Granular Flows” project, which received funding from the Dutch Research Council (NWO) in the framework of the ENW PPP Fund for the top sectors and from the Ministry of Economic Affairs in the framework of the “PPS-Toeslageregeling”.

The authors would like to extend their acknowledgements to dr.ir. Jan van der Stel and dr.ir. Allert Adema from Tata Steel IJmuiden for their invaluable contributions to this review paper.

## References

- Alizadeh M., Hassanpour A., Pasha M., Ghadiri M., Bayly A., The effect of particle shape on predicted segregation in binary powder mixtures, *Powder Technology*, 319 (2017) 313–322. DOI: 10.1016/j.powtec.2017.06.059
- Artega P., Tüzün U., Flow of binary mixtures of equal-density granules in hoppers-size segregation, flowing density and discharge rates, *Chemical Engineering Science*, 45 (1990) 205–223. DOI: 10.1016/0009-2509(90)87093-8
- Asachi M., Behjani M.A., Nourafkan E., Hassanpour A., Tailoring particle shape for enhancing the homogeneity of powder mixtures: experimental study and DEM modelling, *Particuology*, 54 (2021) 58–68. DOI: 10.1016/j.partic.2020.03.006
- Asachi M., Nourafkan E., Hassanpour A., A review of current techniques for the evaluation of powder mixing, *Advanced Powder Technology*, 29 (2018) 1525–1549. DOI: 10.1016/j.apt.2018.03.031
- Barik S.K., Lad V.N., Sreedhar I., Patel C.M., Investigation of mass discharge rate, velocity, and segregation behaviour of microcrystalline cellulose powder from a Copley flow tester, *Powder Technology*, 417 (2023) 118234. DOI: 10.1016/j.powtec.2023.118234
- Bhalode P., Ierapetritou M., A review of existing mixing indices in solid-based continuous blending operations, *Powder Technology*, 373 (2020) 195–209. DOI: 10.1016/j.powtec.2020.06.043
- Bhattacharya T., McCarthy J.J., Chute flow as a means of segregation characterization, *Powder Technology*, 256 (2014) 126–139. DOI: 10.1016/j.powtec.2014.01.092
- Bowler A.L., Bakalis S., Watson N.J., A review of in-line and on-line measurement techniques to monitor industrial mixing processes, *Chemical Engineering Research and Design*, 153 (2020) 463–495. DOI: 10.1016/j.cherd.2019.10.045
- Bridgwater J., Mixing and segregation mechanisms in particle flow, in: Mehta A. (Ed.) *Granular Matter: An Interdisciplinary Approach*, Springer New York, New York, NY, 1994, pp. 161–193, ISBN: 978-1-4612-4290-1.
- Bridgwater J., Cooke M.H., Scott A.M., Interparticle percolation: equipment development and mean percolation velocities, *Transactions of the Institution of Chemical Engineers*, 56 (1978) 157–167.
- Cameron I., Sukhram M., Lefebvre K., Davenport W., *Blast Furnace Ironmaking: Analysis, Control, and Optimization*, Elsevier Inc., 2019, ISBN: 978-0-12-814227-1. DOI: 10.1016/C2017-0-00007-1
- Carson J.W., Royal T.A., Goodwill D.J., Understanding and eliminating particle segregation problems, *Bulk Solids Handling*, 6 (1986) 139–144.
- Chibwe D.K., Evans G.M., Doroodchi E., Monaghan B.J., Pinson D.J., Chew S.J., Charge material distribution behaviour in blast furnace charging system, *Powder Technology*, 366 (2020) 22–35. DOI: 10.1016/j.powtec.2020.02.048
- Cho M., Dutta P., Shim J., A non-sampling mixing index for multicomponent mixtures, *Powder Technology*, 319 (2017) 434–444. DOI: 10.1016/j.powtec.2017.07.011
- Cleary P.W., Sawley M.L., DEM modelling of industrial granular flows: 3D case studies and the effect of particle shape on hopper discharge, *Applied Mathematical Modelling*, 26 (2002) 89–111. DOI: 10.1016/S0307-904X(01)00050-6
- Cliff A., Fullard L.A., Breard E.C.P., Dufek J., Davies C.E., Granular size segregation in silos with and without inserts, *Proceedings of the Royal Society A: Mathematical, Physical and Engineering Sciences*, 477 (2021). 20200242. DOI: 10.1098/rspa.2020.0242
- Coetzee C.J., Calibration of the discrete element method and the effect of particle shape, *Powder Technology*, 297 (2016) 50–70. DOI: 10.1016/j.powtec.2016.04.003
- Coetzee C.J., Review: calibration of the discrete element method, *Powder Technology*, 310 (2017) 104–142. DOI: 10.1016/j.powtec.2017.01.015
- Coetzee C.J., Particle upscaling: calibration and validation of the discrete

- element method, *Powder Technology*, 344 (2019) 487–503. DOI: 10.1016/j.powtec.2018.12.022
- Combarros M., Feise H.J., Zetzener H., Kwade A., Segregation of particulate solids: experiments and DEM simulations, *Particuology*, 12 (2014) 25–32. DOI: 10.1016/j.partic.2013.04.005
- Combarros Garcia M., Feise H.J., Strege S., Kwade A., Segregation in heaps and silos: comparison between experiment, simulation and continuum model, *Powder Technology*, 293 (2016) 26–36. DOI: 10.1016/j.powtec.2015.09.036
- Coulson M., *The History of Mining: The Events, Technology and People Involved in the Industry That Forged the Modern World*, Harriman House Limited, 2012, ISBN: 9781897597903.
- Cundall P.A., Strack O.D.L., A discrete numerical model for granular assemblies, *Geotechnique*, 29 (1979) 47–65. DOI: 10.1680/geot.1979.29.1.47
- de Silva S.R., Dyrøy A., Enstad G.G., Segregation mechanisms and their quantification using segregation testers, in: Rosato A.D., Blackmore D.L. (Eds), *IUTAM Symposium on Segregation in Granular Flows*, Dordrecht, Springer Netherlands, 2000, pp. 11–29. DOI: 10.1007/978-94-015-9498-1\_2
- Do H.Q., Aragón A.M., Schott D.L., A calibration framework for discrete element model parameters using genetic algorithms, *Advanced Powder Technology*, 29 (2018) 1393–1403. DOI: 10.1016/j.apt.2018.03.001
- Drahn J.A., Bridgwater J., The mechanisms of free surface segregation, *Powder Technology*, 36 (1983) 39–53. DOI: 10.1016/0032-5910(83)80007-2
- Duffy S.P., Puri V.M., Primary segregation shear cell for size-segregation analysis of binary mixtures, *KONA Powder and Particle Journal*, 20 (2002) 196–207. DOI: 10.14356/kona.2002022
- El Kassem B., Salloum N., Brinz T., Heider Y., Markert B., A semi-automated dem parameter calibration technique of powders based on different bulk responses extracted from auger dosing experiments, *KONA Powder and Particle Journal*, 38 (2021) 235–250. DOI: 10.14356/kona.2021010
- Gao S., Ottino J.M., Umbanhowar P.B., Lueptow R.M., Modeling granular segregation for overlapping species distributions, *Chemical Engineering Science*, 231 (2021) 116259. DOI: 10.1016/j.ces.2020.116259
- Gao Z., Liu J., Gao T., Advanced inside-furnace monitoring techniques implemented on the new large blast furnace of Shagang, in: *AISTech—Iron and Steel Technology Conference Proceedings*, 2010, pp. 565–571.
- González-Montellano C., Fuentes J.M., Ayuga-Téllez E., Ayuga F., Determination of the mechanical properties of maize grains and olives required for use in DEM simulations, *Journal of Food Engineering*, 111 (2012) 553–562. DOI: 10.1016/j.jfoodeng.2012.03.017
- Gray J.M.N.T., Particle segregation in dense granular flows, *Annual Review of Fluid Mechanics*, 50 (2018) 407–433. DOI: 10.1146/annurev-fluid-122316-045201
- Hong Z., Zhou H., Wu J., Zhan L., Fan Y., Zhang Z., Wu S., Xu H., Wang L.P., Kou M., Effects of operational parameters on particle movement and distribution at the top of a bell-less blast furnace based on discrete element method, *Steel Research International*, 92 (2021) 2000262. DOI: 10.1002/srin.202000262
- Huang A.N., Kuo H.P., Developments in the tools for the investigation of mixing in particulate systems—A review, *Advanced Powder Technology*, 25 (2014) 163–173. DOI: 10.1016/j.apt.2013.10.007
- Huang X., Zheng Q., Liu D., Yu A., Yan W., A design method of hopper shape optimization with improved mass flow pattern and reduced particle segregation, *Chemical Engineering Science*, 253 (2022) 117579. DOI: 10.1016/j.ces.2022.117579
- Izard E., Moreau M., Ravier P., Discrete element method simulation of segregation pattern in a sinter cooler charging chute system, *Particuology*, 59 (2021) 34–42. DOI: 10.1016/j.partic.2020.08.004
- Jain N., Ottino J.M., Lueptow R.M., Regimes of segregation and mixing in combined size and density granular systems: an experimental study, *Granular Matter*, 7 (2005) 69–81. DOI: 10.1007/s10035-005-0198-x
- Jenike A.W., Quantitative design of mass-flow bins, *Powder Technology*, 1 (1967) 237–244. DOI: 10.1016/0032-5910(67)80042-1
- Jin X., Chandratilleke G.R., Wang S., Shen Y., DEM investigation of mixing indices in a ribbon mixer, *Particuology*, 60 (2022) 37–47. DOI: 10.1016/j.partic.2021.03.005
- Jing L., Kwok F.C.Y., Leung A.Y.F., Discrete element modelling of grain size segregation in bi-disperse granular flows down chute, *The 4th International Conference on Particle-based Methods, Fundamentals and Applications (PARTICLES 2015)*, (2015) 474–484. <http://hdl.handle.net/10722/213642>
- Kajiwara Y., Aminaga Y., Inada T., Tanaka T., Sato K. ichi, Size segregation of sinter in the top bunker of a bell-less type blast furnace, *Tetsu-To-Hagane/Journal of the Iron and Steel Institute of Japan*, 74 (1988) 978–984. DOI: 10.2355/tetsutohagane1955.74.6\_978
- Ketterhagen W.R., Curtis J.S., Wassgren C.R., Hancock B.C., Modeling granular segregation in flow from quasi-three-dimensional, wedge-shaped hoppers, *Powder Technology*, 179 (2008) 126–143. DOI: 10.1016/j.powtec.2007.06.023
- Ketterhagen W.R., Curtis J.S., Wassgren C.R., Hancock B.C., Predicting the flow mode from hoppers using the discrete element method, *Powder Technology*, 195 (2009) 1–10. DOI: 10.1016/j.powtec.2009.05.002
- Ketterhagen W.R., Curtis J.S., Wassgren C.R., Kong A., Narayan P.J., Hancock B.C., Granular segregation in discharging cylindrical hoppers: A discrete element and experimental study, *Chemical Engineering Science*, 62 (2007) 6423–6439. DOI: 10.1016/j.ces.2007.07.052
- Ketterhagen W.R., Hancock B.C., Optimizing the design of eccentric feed hoppers for tablet presses using DEM, *Computers and Chemical Engineering*, 34 (2010) 1072–1081. DOI: 10.1016/j.compchemeng.2010.04.016
- Khakhar D.V., McCarthy J.J., Ottino J.M., Mixing and segregation of granular materials in chute flows, *Chaos*, 9 (1999) 594–610. DOI: 10.1063/1.166433
- Kim K.M., Bae J.H., Park J.I., Han J.W., Segregation charging behavior of ultra-fine iron ore briquette in sinter feed bed: DEM analysis, *Metals and Materials International*, 26 (2020) 1218–1225. DOI: 10.1007/s12540-019-00415-y
- Kou M., Wu S., Du K., Shen W., Sun J., Zhang Z., DEM simulation of burden distribution in the upper part of COREX shaft furnace, *ISIJ International*, 53 (2013) 1002–1009. DOI: 10.2355/isijinternational.53.1002
- Kou M., Wu S., Wang G., Zhao B., Cai Q., Numerical simulation of burden and gas distributions inside COREX shaft furnace, *Steel Research International*, 86 (2015) 686–694. DOI: 10.1002/srin.201400311
- Kou M., Xu J., Wu S., Zhou H., Gu K., Yao S., Wen B., Effect of cross-section shape of rotating chute on particle movement and distribution at the throat of a bell-less top blast furnace, *Particuology*, 44 (2019) 194–206. DOI: 10.1016/j.partic.2018.07.010
- Kou M., Xu J., Zhou H., Wen B., Gu K., Yao S., Wu S., Effects of bottom base shapes on burden profiles and burden size distributions in the upper part of a COREX shaft furnace based on DEM, *Advanced Powder Technology*, 29 (2018) 1014–1024. DOI: 10.1016/j.apt.2018.01.020
- Kumar R., Gopireddy S.R., Jana A.K., Patel C.M., Study of the discharge behavior of Rosin-Rammler particle-size distributions from hopper by discrete element method: a systematic analysis of mass flow rate, segregation and velocity profiles, *Powder Technology*, 360 (2020) 818–834. DOI: 10.1016/j.powtec.2019.09.044
- Li C., Honeyands T., O’Dea D., Moreno-Atanasio R., The angle of repose and size segregation of iron ore granules: DEM analysis and experi-

- mental investigation, *Powder Technology*, 320 (2017) 257–272. DOI: 10.1016/j.powtec.2017.07.045
- Li C., Honeyands T., O’Dea D., Moreno-Atanasio R., DEM study on size segregation and voidage distribution in green bed formed on iron ore sinter strand, *Powder Technology*, 356 (2019) 778–789. DOI: 10.1016/j.powtec.2019.09.014
- Li C.X., Dong K.J., Liu S.D., Chandratilleke G.R., Zhou Z.Y., Shen Y.S., DEM study of particle segregation in the throat region of a blast furnace, *Powder Technology*, 407 (2022) 117660. DOI: 10.1016/j.powtec.2022.117660
- Liao H., Zong Y., Li K., Bu Y., Bi Z., Jiang C., Liu Z., Zhang J., Influence of lump ore ratio and shapes on the particle flow behavior inside the direct reduction shaft furnace by discrete element modeling model, *Steel Research International*, 94 (2023) 2200531. DOI: 10.1002/srin.202200531
- Lommen S., Mohajeri M., Lodewijks G., Schott D., DEM particle upscaling for large-scale bulk handling equipment and material interaction, *Powder Technology*, 352 (2019) 273–282. DOI: 10.1016/j.powtec.2019.04.034
- Lommen S., Schott D., Lodewijks G., DEM speedup: Stiffness effects on behavior of bulk material, *Particuology*, 12 (2014) 107–112. DOI: 10.1016/j.partic.2013.03.006
- Lu G., Third J.R., Müller C.R., Discrete element models for non-spherical particle systems: from theoretical developments to applications, *Chemical Engineering Science*, 127 (2015) 425–465. DOI: 10.1016/j.ces.2014.11.050
- Luding S., Introduction to discrete element methods: basic of contact force models and how to perform the micro-macro transition to continuum theory, *European Journal of Environmental and Civil Engineering*, 12 (2008) 785–826. DOI: 10.1080/19648189.2008.9693050
- Mandal S., Khakhar D.V., Dense granular flow of mixtures of spheres and dumbbells down a rough inclined plane: segregation and rheology, *Physics of Fluids*, 31 (2019) 23304. DOI: 10.1063/1.5082355
- Mantravadi B., Tan D.S., Effect of bend angle on granular size segregation in the chute flow under periodic flow inversion, *Powder Technology*, 360 (2020) 177–192. DOI: 10.1016/j.powtec.2019.10.005
- Marigo M., Stitt E.H., Discrete element method (DEM) for industrial applications: comments on calibration and validation for the modelling of cylindrical pellets, *KONA Powder and Particle Journal*, 32 (2015) 236–252. DOI: 10.14356/kona.2015016
- Mio H., Kadowaki M., Matsuzaki S., Kunitomo K., Development of particle flow simulator in charging process of blast furnace by discrete element method, *Minerals Engineering*, 33 (2012) 27–33. DOI: 10.1016/j.mineng.2012.01.002
- Mio H., Komatsuki S., Akashi M., Shimosaka A., Shirakawa Y., Hidaka J., Kadowaki M., Matsuzaki S., Kunitomo K., Validation of particle size segregation of sintered ore during flowing through laboratory-scale chute by discrete element method, *ISIJ International*, 48 (2008a) 1696–1703. DOI: 10.2355/isijinternational.48.1696
- Mio H., Komatsuki S., Akashi M., Shimosaka A., Shirakawa Y., Hidaka J., Kadowaki M., Matsuzaki S., Kunitomo K., Validation of particle size segregation of sintered ore during flowing through laboratory-scale chute by discrete element method, *ISIJ International*, 48 (2008b) 1696–1703. DOI: 10.2355/isijinternational.48.1696
- Mio H., Komatsuki S., Akashi M., Shimosaka A., Shirakawa Y., Hidaka J., Kadowaki M., Matsuzaki S., Kunitomo K., Effect of chute angle on charging behavior of sintered ore particles at bell-less type charging system of blast furnace by discrete element method, *ISIJ International*, 49 (2009) 479–486. DOI: 10.2355/isijinternational.49.479
- Mio H., Komatsuki S., Akashi M., Shimosaka A., Shirakawa Y., Hidaka J., Kadowaki M., Yokoyama H., Matsuzaki S., Kunitomo K., Analysis of traveling behavior of nut coke particles in bell-type charging process of blast furnace by using discrete element method, *ISIJ International*, 50 (2010) 1000–1009. DOI: 10.2355/isijinternational.50.1000
- Mio H., Narita Y., Nakano K., Nomura S., Validation of the burden distribution of the 1/3-scale of a blast furnace simulated by the discrete element method, *Processes*, 8 (2020) 6. DOI: 10.3390/pr8010006
- Mohajeri M.J., Do H.Q., Schott D.L., DEM calibration of cohesive material in the ring shear test by applying a genetic algorithm framework, *Advanced Powder Technology*, 31 (2020) 1838–1850. DOI: 10.1016/j.aapt.2020.02.019
- Muzzio F.J., Robinson P., Wightman C., Dean Brone, Sampling practices in powder blending, *International Journal of Pharmaceutics*, 155 (1997) 153–178. DOI: 10.1016/S0378-5173(97)04865-5
- Nadeem H., Heindel T.J., Review of noninvasive methods to characterize granular mixing, *Powder Technology*, 332 (2018) 331–350. DOI: 10.1016/j.powtec.2018.03.035
- Nakano M., Abe T., Kano J., Kunitomo K., DEM analysis on size segregation in feed bed of sintering machine, *ISIJ International*, 52 (2012) 1559–1564. DOI: 10.2355/isijinternational.52.1559
- Ottino J.M., Khakhar D.V., Mixing and segregation of granular materials, *Annual Review of Fluid Mechanics*, 32 (2000) 55–91. DOI: 10.1146/annurev.fluid.32.1.55
- Panda S., Tan D.S., Effect of external factors on segregation of different granular mixtures, *Advanced Powder Technology*, 31 (2020a) 571–594. DOI: 10.1016/j.aapt.2019.11.013
- Panda S., Tan D.S., Study of external factors to minimize segregation of granular particles, *International Journal of Modern Physics C*, 31 (2020b) 2050147. DOI: 10.1142/S0129183120501478
- Pereira G.G., Cleary P.W., De-mixing of binary particle mixtures during unloading of a V-blender, *Chemical Engineering Science*, 94 (2013) 93–107. DOI: 10.1016/j.ces.2013.02.051
- Qiu P., Pabst T., Waste rock segregation during disposal: calibration and upscaling of discrete element simulations, *Powder Technology*, 412 (2022) 117981. DOI: 10.1016/j.powtec.2022.117981
- Rhodes M., Introduction to Particle Technology, 2nd edition, John Wiley & Sons, 2008, ISBN: 9780470014271. DOI: 10.1002/9780470727102
- Richard P., Nicodemi M., Delannay R., Ribière P., Bideau D., Slow relaxation and compaction of granular systems, *Nature Materials*, 4 (2005) 121–128. DOI: 10.1038/nmat1300
- Roessler T., Katterfeld A., Scaling of the angle of repose test and its influence on the calibration of DEM parameters using upscaled particles, *Powder Technology*, 330 (2018) 58–66. DOI: 10.1016/j.powtec.2018.01.044
- Roessler T., Richter C., Katterfeld A., Will F., Development of a standard calibration procedure for the DEM parameters of cohesionless bulk materials – part I: Solving the problem of ambiguous parameter combinations, *Powder Technology*, 343 (2019) 803–812. DOI: 10.1016/j.powtec.2018.11.034
- Rosato A., Windows-Yule C., Segregation in Vibrated Granular Systems, Elsevier Inc., 2020, ISBN: 9780128141991. DOI: 10.1016/C2017-0-00407-X
- Sakai M., How should the discrete element method be applied in industrial systems?: a review, *KONA Powder and Particle Journal*, 33 (2016) 169–178. DOI: 10.14356/kona.2016023
- Saleh K., Golshan S., Zarghami R., A review on gravity flow of free-flowing granular solids in silos – Basics and practical aspects, *Chemical Engineering Science*, 192 (2018) 1011–1035. DOI: 10.1016/j.ces.2018.08.028
- Schulze D., *Powders and Bulk Solids: Behavior, Characterization, Storage and Flow*, Springer Berlin, 2008, ISBN: 978-3-540-73767-4. DOI: 10.1007/978-3-540-73768-1
- Seil P., Gómez J.O., Pirker S., Kloss C., Numerical and experimental studies on segregation patterns in granular flow from two hoppers, in: *ECCOMAS 2012—European Congress on Computational Methods in Applied Sciences and Engineering*, E-Book Full Papers, 2012, pp. 5389–5402.
- Shekhar S., Pereira G.G., Hapgood K.P., Morton D.A.V., Cleary P.W., Simulation study on the influence of particle properties on radial and axial segregation in a Freeman rheometer, *Chemical Engineering*

- Science, 265 (2023) 118210. DOI: 10.1016/j.ces.2022.118210
- Shenoy P., Innings F., Tammel K., Fitzpatrick J., Ahmé L., Evaluation of a digital colour imaging system for assessing the mixture quality of spice powder mixes by comparison with a salt conductivity method, Powder Technology, 286 (2015) 48–54. DOI: 10.1016/j.powtec.2015.07.034
- Shi D., Abatan A.A., Vargas W.L., McCarthy J.J., Eliminating segregation in free-surface flows of particles, Physical Review Letters, 99 (2007) 148001. DOI: 10.1103/PhysRevLett.99.148001
- Shimosaka A., Shirakawa Y., Hidaka J., Effects of particle shape and size distribution on size segregation of particles, Journal of Chemical Engineering of Japan, 46 (2013) 187–195. DOI: 10.1252/jcej.12we179
- Shirsath S.S., Padding J.T., Kuipers J.A.M., Clercx H.J.H., Simulation study of the effect of wall roughness on the dynamics of granular flows in rotating semicylindrical chutes, AIChE Journal, 61 (2015) 2117–2135. DOI: 10.1002/aic.14828
- Shlnohara K., Mlyata S.I., Mechanism of density segregation of particles in filling vessels, Industrial and Engineering Chemistry Process Design and Development, 23 (1984) 423–428. DOI: 10.1021/i200026a003
- Soltanbeigi B., Podlozhnyuk A., Papanicolopoulos S.A., Kloss C., Pirker S., Ooi J.Y., DEM study of mechanical characteristics of multi-spherical and superquadric particles at micro and macro scales, Powder Technology, 329 (2018) 288–303. DOI: 10.1016/j.powtec.2018.01.082
- Standish N., Studies of size segregation in filling and emptying a hopper, Powder Technology, 45 (1985) 43–56. DOI: 10.1016/0032-5910(85)85059-2
- Standish N., Kilic A., Comparison of stop-start and continuous sampling methods of studying segregation of materials discharging from a hopper, Chemical Engineering Science, 40 (1985) 2152–2153. DOI: 10.1016/0009-2509(85)87036-6
- Stannarius R., Magnetic resonance imaging of granular materials, The Review of scientific instruments, 88 (2017) 51806. DOI: 10.1063/1.4983135
- Tang P., Puri V.M., Methods for minimizing segregation: a review, Particulate Science and Technology, 22 (2004) 321–337. DOI: 10.1080/02726350490501420
- Tang P., Puri V.M., An innovative device for quantification of percolation and sieving segregation patterns—Single component and multiple size fractions, Particulate Science and Technology, 23 (2005) 335–350. DOI: 10.1080/02726350500212871
- Tao H., Zhong W., Jin B., Ren B., DEM simulation of non-spherical granular segregation in hopper, AIP Conference Proceedings, American Institute of Physics, 1547 (2013) 720–726. DOI: 10.1063/1.4816925
- Terui K., Kashihara Y., Hirokawa T., Nouchi T., Optimization of coke mixed charging based on discrete element method, ISIJ International, 57 (2017) 1804–1810. DOI: 10.2355/isijinternational.ISIJINT-2017-204
- Tian X., Zhou H., Huang J., Wu S., Wang G., Kou M., DEM study on discharge behavior of ternary cylindrical activated coke particles, Powder Technology, 409 (2022) 117785. DOI: 10.1016/j.powtec.2022.117785
- Tripathi A., Khakhar D. V., Rheology of binary granular mixtures in the dense flow regime, Physics of Fluids, 23 (2011) 113302. DOI: 10.1063/1.3653276
- Tripathi A., Khakhar D. V., Density difference-driven segregation in a dense granular flow, Journal of Fluid Mechanics, 717 (2013) 643–669. DOI: 10.1017/jfm.2012.603
- Vallance J.W., Savage S.B., Particle segregation in granular flows down chutes, in: Rosato A.D., Blackmore D.L. (Eds), IUTAM Symposium on Segregation in Granular Flows, Dordrecht, Springer Netherlands, 2000, pp. 31–51. DOI: 10.1007/978-94-015-9498-1\_3
- Vuiloz T., Cantor D., Ovalle C., DEM modeling of segregation and stratification in pouring heaps of bidispersed mixtures of rounded particles, EPJ Web of Conferences, 249 (2021) 3049. DOI: 10.1051/epjconf/202124903049
- Wang C., Deng A., Taheri A., Digital image processing on segregation of rubber sand mixture, International Journal of Geomechanics, 18 (2018) 4018138. DOI: 10.1061/(asce)gm.1943-5622.0001269
- Wang M., Liang L.-x., Guan S.-h., Ma G., Lai Z.-q., Niu X.-q., Zhang S.-f., Tian W.-x., Zhou W., Experimental and numerical investigation of the collapse of binary mixture of particles with different densities, Powder Technology, 415 (2023) 118167. DOI: 10.1016/j.powtec.2022.118167
- Wang X., Ma H., Li B., Li T., Xia R., Bao Q., Review on the research of contact parameters calibration of particle system, Journal of Mechanical Science and Technology, 36 (2022) 1363–1378. DOI: 10.1007/s12206-022-0225-4
- Wensrich C.M., Katterfeld A., Rolling friction as a technique for modeling particle shape in DEM, Powder Technology, 217 (2012) 409–417. DOI: 10.1016/j.powtec.2011.10.057
- Williams J., Mixing and segregation in powders, in: M.J. Rhodes(ed.), Principles of Powder Technology, John Wiley & Sons, 1991, pp. 71–90, ISBN: 978-0-471-92422-7
- Williams J.C., The segregation of particulate materials. A review, Powder Technology, 15 (1976) 245–251. DOI: 10.1016/0032-5910(76)80053-8
- Wu S., Kou M., Xu J., Guo X., Du K., Shen W., Sun J., DEM simulation of particle size segregation behavior during charging into and discharging from a Paul-Wurth type hopper, Chemical Engineering Science, 99 (2013) 314–323. DOI: 10.1016/j.ces.2013.06.018
- Xu J., Hu Z., Xu Y., Wang D., Wen L., Bai C., Transient local segregation grids of binary size particles discharged from a wedge-shaped hopper, Powder Technology, 308 (2017) 273–289. DOI: 10.1016/j.powtec.2016.12.013
- Xu W., Cheng S., Li C., Experimental study of the segregation of burden distribution during the Charging Process of Bell-less Top Blast Furnace with Two Parallel Hoppers, in: Journal of Physics: Conference Series, Taylor & Francis, 2021, pp. 337–343. DOI: 10.1088/1742-6596/2044/1/012129
- Xu W., Cheng S., Niu Q., Hu W., Bang J., Investigation on the uneven distribution of different types of ores in the hopper and stock surface during the charging process of blast furnace based on discrete element method, Metallurgical Research and Technology, 116 (2019) 314. DOI: 10.1051/metal/2018099
- Xu Y., Ma K., Sun C., Liao Z., Xu J., Wen L., Bai C., Effect of density difference on particle segregation behaviors at bell-less top blast furnace with parallel-type hopper, in: Minerals, Metals and Materials Series, Springer, 2018a, pp. 391–399. DOI: 10.1007/978-3-319-72138-5\_39
- Xu Y., Xu J., Sun C., Ma K., Shan C., Wen L., Zhang S., Bai C., Quantitative comparison of binary particle mass and size segregation between serial and parallel type hoppers of blast furnace bell-less top charging system, Powder Technology, 328 (2018b) 245–255. DOI: 10.1016/j.powtec.2018.01.020
- Yang W., Zhou Z., Pinson D., Yu A., Periodic boundary conditions for discrete element method simulation of particle flow in cylindrical vessels, Industrial and Engineering Chemistry Research, 53 (2014) 8245–8256. DOI: 10.1021/ie404158e
- Yang W.J., Zhou Z.Y., Yu A.B., Discrete particle simulation of solid flow in a three-dimensional blast furnace sector model, Chemical Engineering Journal, 278 (2015) 339–352. DOI: 10.1016/j.ccej.2014.11.144
- You Y., Hou Q.F., Luo Z.G., Li H.F., Zhou H., Chen R., Zou Z.S., Three-dimensional DEM study of coal distribution in the melter gasifier of COREX, Steel Research International, 87 (2016) 1543–1551. DOI: 10.1002/srin.201500481

Yu F., Zhang Y., Zheng Y., Han M., Chen G., Yao Z., Comparison of different effective diameter calculating methods for spherocylinders by geometrically exact DEM simulations, *Powder Technology*, 360 (2020) 1092–1101. DOI: 10.1016/j.powtec.2019.10.097

Yu Y., Saxén H., Experimental and DEM study of segregation of ternary size particles in a blast furnace top bunker model, *Chemical Engineering Science*, 65 (2010) 5237–5250. DOI: 10.1016/j.ces.2010.06.025

Yu Y., Saxén H., Flow of pellet and coke particles in and from a fixed chute, *Industrial and Engineering Chemistry Research*, 51 (2012) 7383–7397. DOI: 10.1021/ie201362n

Yu Y., Saxén H., Particle flow and behavior at bell-less charging of the blast furnace, *Steel Research International*, 84 (2013) 1018–1033. DOI: 10.1002/srin.201300028

Yu Y., Saxén H., Segregation behavior of particles in a top hopper of a blast furnace, *Powder Technology*, 262 (2014) 233–241. DOI: 10.1016/j.powtec.2014.04.010

Yu Y., Zhang J., Zhang J., Saxén H., DEM and experimental studies on pellet segregation in stockpile build-up, *Ironmaking and Steelmaking*, 45 (2018) 264–271. DOI: 10.1080/03019233.2016.1261244

Zhang D., Zhou Z., Pinson D., DEM simulation of particle stratification and segregation in stockpile formation, *EPJ Web of Conferences*, 140 (2017) 15018. DOI: 10.1051/epjconf/201714015018

Zhang J., Hu Z., Ge W., Zhang Y., Li T., Li J., Application of the discrete approach to the simulation of size segregation in granular chute flow, *Industrial and Engineering Chemistry Research*, 43 (2004) 5521–5528. DOI: 10.1021/ie034254f

Zhang J., Qiu J., Guo H., Ren S., Sun H., Wang G., Gao Z., Simulation of particle flow in a bell-less type charging system of a blast furnace using the discrete element method, *Particuology*, 16 (2014) 167–177. DOI: 10.1016/j.partic.2014.01.003

Zhang T.F., Gan J.Q., Pinson D., Zhou Z.Y., Size-induced segregation of granular materials during filling a conical hopper, *Powder Technology*, 340 (2018) 331–343. DOI: 10.1016/j.powtec.2018.09.031

Zhang T.F., Gan J.Q., Yu A.B., Pinson D., Zhou Z.Y., Segregation of granular binary mixtures with large particle size ratios during hopper discharging process, *Powder Technology*, 361 (2020) 435–445. DOI: 10.1016/j.powtec.2019.07.010

Zhang T.F., Gan J.Q., Yu A.B., Pinson D., Zhou Z.Y., Size segregation of granular materials during Paul-Wurth hopper charging and discharging process, *Powder Technology*, 378 (2021) 497–509. DOI: 10.1016/j.powtec.2020.10.025

Zhang Z., Liu Y., Zheng B., Sun P., Li R., Local percolation of a binary particle mixture in a rectangular hopper with inclined bottom during discharging, *ACS Omega*, 5 (2020) 20773–20783. DOI: 10.1021/acsomega.0c01514

Zhao Y., Chew J.W., Discrete element method study on hopper discharge behaviors of binary mixtures of nonspherical particles, *AIChE Journal*, 66 (2020a) e16254. DOI: 10.1002/aic.16254

Zhao Y., Chew J.W., Effect of lognormal particle size distributions of non-spherical particles on hopper discharge characteristics, *Chemical Engineering Research and Design*, 163 (2020b) 230–240. DOI: 10.1016/j.cherd.2020.09.001

Zhao Y., Luo Y., Wang W., Liu S., Zhan Z., Effect of base roughness on flow behaviour and size segregation in dry granular flows, *Geotechnique Letters*, 12 (2022) 258–264. DOI: 10.1680/jgele.22.00044

Zhao Y., Yang S., Zhang L., Chew J.W., DEM study on the discharge characteristics of lognormal particle size distributions from a conical hopper, *AIChE Journal*, 64 (2018) 1174–1190. DOI: 10.1002/aic.16026

Zhu H.P., Zhou Z.Y., Yang R.Y., Yu A.B., Discrete particle simulation of particulate systems: theoretical developments, *Chemical Engineering Science*, 62 (2007) 3378–3396. DOI: 10.1016/j.ces.2006.12.089

## Appendix

In **Table 2**, we summarized the segregation indices used in the literature. These indices quantify to which degree the tracer particle is homogeneously distributed within the mixture. For indices no. 1–8, the concentration of tracer

particles is determined in each sub-domain, which can be expressed in terms of the number, mass or volume fraction, as indicated in **Table A1**.

**Table A1** Equations for calculating the concentration of different types of particles (type-A or type-B) on number, mass and volume basis. Legend:  $N$  = number of particles,  $m$  = mass of particles,  $V$  = volume of particles.

	Number-based	Mass-based	Volume-based
Fraction of particle type-A	$(\phi_N)_A = \frac{N_A}{N}$ where $N = N_A + N_B$	$(\phi_m)_A = \frac{m_A}{m}$ where $m = m_A + m_B$	$(\phi_V)_A = \frac{V_A}{V}$ where $V = V_A + V_B$
Fraction of particle type-B	$(\phi_N)_B = \frac{N_B}{N}$	$(\phi_m)_B = \frac{m_B}{m}$	$(\phi_V)_B = \frac{V_B}{V}$
Total (number/mass/volume) fraction	$\phi_N = (\phi_N)_A + (\phi_N)_B = 1$	$\phi_m = (\phi_m)_A + (\phi_m)_B = 1$	$\phi_V = (\phi_V)_A + (\phi_V)_B = 1$
Relative fraction of tracer particle in bin $i$	$y_t^i = \frac{(\phi_N)_t^i}{\phi_N} = (\phi_N)_t^i$ where $t = A$ or $B$	$x_t^i = \frac{(\phi_m)_t^i}{\phi_m} = (\phi_m)_t^i$ where $t = A$ or $B$	$c_t^i = \frac{(\phi_V)_t^i}{\phi_V}$ where $t = A$ or $B$
Relative fraction of tracer particle in the entire system	$y_t = \frac{(\phi_N)_t}{\phi_N} = (\phi_N)_t$ where $t = A$ or $B$	$x_t = \frac{(\phi_m)_t}{\phi_m} = (\phi_m)_t$ where $t = A$ or $B$	$c_t = \frac{(\phi_V)_t}{\phi_V}$ where $t = A$ or $B$

## Authors' Short Biographies



### Ahmed Hadi

Ahmed Hadi earned a BSc in Civil Engineering from Isfahan University of Technology in 2015. He then pursued an MSc in Geotechnical Engineering at the University of Tehran, graduating in 2018. During his master's degree, he specialised in the DEM modelling of shear banding in granular soils. Currently, Ahmed Hadi is a PhD candidate at the GranChaMlab@TUDelft. His current research project focuses on the DEM modelling of multi-component segregation in the blast furnace charging system.



### Raïsa Roeplal

Raïsa Roeplal pursued a master's degree in Mechanical Engineering at the University of Twente in 2016. During that time, she studied the mixing of cohesive particles in paddle mixers and became fascinated with the segregation behaviour of granular materials. She joined the GranChaMlab@TUDelft at Delft University of Technology in 2020, in pursuit of her PhD degree. She is currently developing a DEM model to study the flow and packing behaviour of blast furnace mixtures during furnace charging. Her main focus areas in this regard are: high-velocity dense granular flows, industrial granular flow modelling, multi-component segregation and mixture calibration.



### Yusong Pang

Yusong Pang received his MSc degree in Electrical Engineering in 1996. In 2000 he started working at Practic B.V. and Seaview B.V., the Netherlands, for industrial production life cycle management. After his PhD research of intelligent belt conveyor monitoring and control in 2007, he was employed by the Advisory Group Industrial Installations of Royal Haskoning, the Netherlands, as an expert in material handling. In 2010 he was appointed Assistant Professor in the section of Transport Engineering and Logistics, Delft University of Technology, the Netherlands. His research focuses on the intelligent control for large-scale material handling systems and logistics processes.



### Dingena Schott

Dingena Schott is a Full Professor at TU Delft on Machine Cargo Interaction Engineering. She obtained her PhD in 2004 from TU Delft on the homogenisation of bulk materials in mammoth silos. In 2007 she started the GranChaMlab@TUDelft to characterise, model, calibrate and validate granular materials for enabling the simulation-supported design of cargo handling equipment on an industrial scale. Since then, she has worked on developing calibration frameworks and modelling particle-based systems in various design contexts; including terminal designs for particulate materials, as well as an award-winning new grab design. Her main research interests include: machine-cargo interfaces, simulation-supported design, biomass materials and energy-transition-driven handling and logistics.